

## **INFORMATION TO USERS**

This manuscript has been reproduced from the microfilm master. UMI films the text directly from the original or copy submitted. Thus, some thesis and dissertation copies are in typewriter face, while others may be from any type of computer printer.

**The quality of this reproduction is dependent upon the quality of the copy submitted.** Broken or indistinct print, colored or poor quality illustrations and photographs, print bleedthrough, substandard margins, and improper alignment can adversely affect reproduction.

In the unlikely event that the author did not send UMI a complete manuscript and there are missing pages, these will be noted. Also, if unauthorized copyright material had to be removed, a note will indicate the deletion.

Oversize materials (e.g., maps, drawings, charts) are reproduced by sectioning the original, beginning at the upper left-hand corner and continuing from left to right in equal sections with small overlaps.

Photographs included in the original manuscript have been reproduced xerographically in this copy. Higher quality 6" x 9" black and white photographic prints are available for any photographs or illustrations appearing in this copy for an additional charge. Contact UMI directly to order.

**Bell & Howell Information and Learning  
300 North Zeeb Road, Ann Arbor, MI 48106-1346 USA**

**UMI<sup>®</sup>**  
**800-521-0600**



# **A Study of High Wind Storms Affecting Atlantic Canada, 1979-1995**

by  
**Shawn S. Allan**

**Department of Atmospheric And Oceanic Sciences  
McGill University, Montreal**

**June 1998**

**A thesis submitted to the Faculty of Graduate Studies and Research in partial fulfillment of the  
requirements of the degree of Master of Science.**

**© Shawn Stanley Allan 1998**



National Library  
of Canada

Acquisitions and  
Bibliographic Services

395 Wellington Street  
Ottawa ON K1A 0N4  
Canada

Bibliothèque nationale  
du Canada

Acquisitions et  
services bibliographiques

395, rue Wellington  
Ottawa ON K1A 0N4  
Canada

*Your file* *Votre référence*

*Our file* *Notre référence*

The author has granted a non-exclusive licence allowing the National Library of Canada to reproduce, loan, distribute or sell copies of this thesis in microform, paper or electronic formats.

The author retains ownership of the copyright in this thesis. Neither the thesis nor substantial extracts from it may be printed or otherwise reproduced without the author's permission.

L'auteur a accordé une licence non exclusive permettant à la Bibliothèque nationale du Canada de reproduire, prêter, distribuer ou vendre des copies de cette thèse sous la forme de microfiche/film, de reproduction sur papier ou sur format électronique.

L'auteur conserve la propriété du droit d'auteur qui protège cette thèse. Ni la thèse ni des extraits substantiels de celle-ci ne doivent être imprimés ou autrement reproduits sans son autorisation.

0-612-44114-8

## Abstract

A climatology of high wind events (HWEs) affecting Sable Island (44°N, 60°W) and Halifax (44.5°N, 63.5°W) was constructed for the period 1979-1995. We then focussed on HWEs at Sable Island in more detail because of their high frequency relative to Halifax. Events were stratified into four groups based on the direction of the peak speed: NE (1°-90°), SE (91°-180°), SW (181°-270°), and NW (271°-360°). Synoptic structures and statistically significant atmospheric anomalies were identified in composites for each group. More detailed structures were found in composites constructed with the aid of a cluster analysis.

*NW HWEs* were associated with rapidly deepening marine cyclones and lacked clear atmospheric predecessors. *NE HWEs* were linked to a slow moving offshore cyclone and prominent anticyclone near Labrador. An anomalously weak Icelandic Low was a dominant precursor signal and an important feature found in each of the groups. *SE HWEs* were related to the strong pressure gradient between a cyclone-anticyclone couplet. The anticyclone was evident four days before the *HWE* and played a crucial role in the development of the cyclone. *SW HWEs* were related to a variety of cyclone types, but were typically related to a low-frequency cold surge over eastern North America.

The storms most difficult to predict may be *NW HWEs*, since they lack clear atmospheric precursor signals. They are also among the most dangerous storms affecting Atlantic Canada, since they move and develop rapidly, and have some of the highest wind speeds.

## Résumé

Une climatologie des événements de vent intense (EVI) affectant Sable Island (44°N, 60°W) et Halifax (44.5°N, 63.5°W) a été élaborée pour la période 1979-1995. Notre attention a ensuite été portée vers les EVIs de Sable Island à cause de leur fréquence plus élevée que ceux d'Halifax. Les événements ont été séparés en quatre groupes selon la direction de leur vitesse maximale: NE (1°-90°), SE (91°-180°), SW (181°-270°), and NW (271°-360°). Les structures synoptiques et les anomalies atmosphériques statistiquement significatives ont été identifiées dans des champs composés pour chaque groupe. Des structures plus détaillées ont été découvertes dans des champs composés construits à l'aide d'une analyse de groupe.

Les *EVIs NW* ont été associés à des cyclones marins s'intensifiant rapidement et étaient dépourvus de prédécesseurs atmosphériques précis. Les *EVIs NE* ont été associés à un cyclone se déplaçant lentement au large et à un anticyclone important près du Labrador. Une circulation anormalement faible à proximité de la Basse Pression Islandaise (Icelandic Low) en était un signal précurseur dominant. Les *EVIs SE* sont reliés au fort gradient de pression d'un couple cyclone-anticyclone. L'anticyclone est présent quatre jours avant l'EVI et joue un rôle critique dans le développement du cyclone. Les *EVIs SW* sont associés à une variété de types de cyclones mais sont typiquement reliés à une vague d'air froid de basse fréquence au-dessus de la partie est de l'Amérique du Nord.

Il appert qu'une circulation affaiblie au-dessus de l'océan Atlantique est un facteur important qui favorise l'apparition de l'EVI. De plus, les *EVIs NW* apparaissent comme étant les plus difficiles à prédire puisqu'ils ne possèdent pas de signaux atmosphériques précurseurs précis, se déplacent rapidement et possèdent les vitesses éoliennes les plus élevées.

## Acknowledgements

This research has been sponsored by research grants from the Natural Sciences and Engineering Research Council, Atmospheric Environment Service (AES) of Canada, and the Quebec Fonds pour la Formation de Chercheurs et l'Aide à la Recherche. Additional support has been provided by an AES research contract. Special thanks go to Jim Abraham of the AES Maritimes Weather Centre for providing valuable data and technical assistance in this work.

I would like to thank my thesis supervisor, Dr. John R. Gyakum, for his guidance and support during this project, and especially for allowing me to pursue my interest in the Atlantic Canada region. I also appreciate his encouragement and financial support in allowing me to present my work at conferences in Saratoga Springs, NY, and Dartmouth, NS.

Thanks are extended to Alex Fischer for his help in getting me started at a time when 'C-shell' and UNIX were about as familiar to me as Latin. Werner Wintels and Marco Carrera have also been very helpful in providing constructive criticism and suggestions related to my research. The technical support on software by Will Cheng and writing of the French version of the abstract by Louis-Phillipe Crevier are greatly appreciated.

I would like to thank Jason Milbrant for his many hours of discussion on a variety of meteorological topics and the coffee breaks that frequently provided the mental stimulus to continue.

Thank you, Dad and Mum, for more than can be expressed in words. Most importantly, I would like to thank the Lord Jesus for making these two years possible.

## Table of Contents

Abstract	i
Résumé	ii
Acknowledgements	iii
Table of Contents	iv
<b>Chapter 1 Introduction</b>	
1.1 Motivation	1
1.2 Weather systems affecting eastern North America and the Atlantic Canada region	2
1.3 Objectives	5
<b>Chapter 2 Data sets and analysis procedures</b>	
2.1 Data	8
2.2 Analysis of wind data	9
2.3 Composite methodology	10
2.4 Linear correlation analysis	11
2.5 Cyclone tracks	12
<b>Chapter 3 Climatology of high wind events for the period 1979-1995</b>	
3.1 Interannual and monthly variability of high wind events	14
3.2 The contrasting periods of January 1982 and January 1984	16
3.3 Categorising high wind events by wind direction	22
<b>Chapter 4 Planetary- and synoptic-scale structure associated with high wind events at Sable Island</b>	
4.1 Introduction	31
4.2 The northeast quadrant	33
4.3 The southeast quadrant	40
4.4 The southwest quadrant	48
4.5 The northwest quadrant	57
<b>Chapter 5 Summary and conclusions</b>	
5.1 Summary	65
5.2 Conclusions	70
Bibliography	71



# Chapter 1 - Introduction

## 1.1 Motivation

Perhaps the most dangerous aspect of weather systems at sea are the associated high winds. These are a threat to shipping and pose grave danger to human life. An extreme example was the Ocean Ranger storm of 12-15 February 1982, which was responsible for the deaths of 117 crewmen when the oil rig *Ocean Ranger* and nearby freighter *Mekhanik Tarasov* sank in heavy seas (Kuo et al. 1991). Sable Island (44°N 60°W) reported gusts of up to  $49 \text{ m s}^{-1}$  associated with this storm.

The physical processes preceding and favouring explosive cyclogenesis have received a great deal of attention over the last several years through composite (e.g., Rogers and Bosart 1986; Manobianco 1989), modelling (e.g., Balasubramanian and Yau 1994; Rausch and Smith 1996), and individual case studies (e.g., Gyakum 1983a,b; Roebber 1993). Some studies have shown that distinctive signatures can be found in the atmosphere several days before the occurrence of a rapidly deepening cyclone. Lackmann et al. (1996) and Sanders and Davis (1988) showed that large-scale signatures may precede explosive cyclogenesis over the western Atlantic Ocean up to four days beforehand. Konrad (1996) found that planetary-scale circulation anomalies are strongly related to the intensity of cold air outbreaks and suggested, in agreement with Konrad and Colucci (1989), that there is evidence to link these cold air outbreaks to the occurrence of explosive cyclogenesis along the United States east coast.

These findings support a strong connection between the large-scale atmospheric circulation and increased frequency and intensity of explosive cyclones along the east coast of North America. However, explosive cyclones are not the only weather systems capable of delivering high winds and a more complete study of all dangerous storms is needed to benefit those who are at risk from them. One example of a destructive storm which did not deepen explosively but which affected a large part of the east coast of North America was the storm of 28-31 October 1991. This was responsible for the sinking of two ships and billions of dollars of damage from Nova Scotia to the Bahamas (Avila and Pasch 1992; Davis and Dolan 1992). More work is needed to document large-scale circulation anomalies favouring the development of high wind storms. This would

help to establish whether there is a chance of improving the long range probability forecast of particularly violent weather systems.

## **1.2 Weather systems affecting eastern North America and the Atlantic Canada region**

The most common weather systems posing a threat to eastern coastal regions of North America are extratropical cyclones. It is a well established fact that there is a pronounced maximum in cyclone frequency in ocean waters off the east coast of Canada and the United States during the cold season (e.g., Petterssen 1956; Sanders and Gyakum 1980; Roebber 1984). Sanders and Gyakum (1980) defined a bomb as a cyclone whose central pressure fell at least  $1 \text{ hPa h}^{-1}$  for 24 h, adjusted for latitude by multiplying this rate by  $\sin\phi/\sin 60$  at some latitude  $\phi$ . These authors studied bombs in the Northern Hemisphere between September 1976 and May 1979. They found that bombs are primarily maritime events with a pronounced frequency maximum over the Atlantic and Pacific Ocean, within or just north of the Gulf Stream and Kuroshio currents, respectively. They also found that although there was a higher frequency over the Pacific Ocean, more than twice as many extreme bombs occurred over the Atlantic Ocean. Roebber (1984) updated this climatology to include the 1979-1982 cold seasons, while also including all extratropical cyclones which were not "bombs". He found similar results to Sanders and Gyakum (1980), with a maximum in formation positions over the south-eastern United States, along the lee of the Rocky mountains and just east of Newfoundland. Maximum deepening occurred over the western Atlantic in an area extending from the coast of Georgia north-eastward to Newfoundland.

Some well known examples of explosive cyclones in the western Atlantic include the Presidents' Day snowstorm of February 1979 (Bosart 1981; Bosart and Lin 1984; Uccellini et al. 1984) and the Queen Elizabeth II storm of September 1978 (Gyakum 1983a,b; Uccellini 1986). These and other studies have suggested that an important component of rapid cyclogenesis is the baroclinic mechanism, where rapid development is triggered as an upper-level trough moves over a low-level baroclinic zone (Reed and Albright 1986, Uccellini 1986; Manobianco 1989; Rogers and Bosart 1986). Deepening is facilitated through physical mechanisms such as surface sensible and latent heat fluxes

acting to decrease the static stability in the presence of strong surface-air temperature contrast (Gyakum 1983b; Bosart and Lin 1984). Others have suggested the importance of latent heat release in enhancing a cyclone's development (Zhang and MacGillivray 1997; Uccellini et al. 1987).

As stated previously, explosive development has been linked to large-scale circulation anomalies in a number of studies. Dickson and Namais (1976) noticed that alterations in the pressure anomaly cell in the Greenland-Iceland area had important effects on the winter climate of Europe. They proposed that the establishment of these sustained pressure anomaly cells was linked to explosive development along the main coastal baroclinic zone of eastern North America. Anomalously cold winters are characterised by enhanced coastal baroclinicity effecting more rapid development of explosive cyclones to occlusion, south-west of their normal resting place in the vicinity of the climatological Icelandic Low. This would set up a southerly flow east of Greenland, acting to sustain and anchor the ridge anomaly in that region. When Dickson and Namais (1976) examined colder than normal winters over the eastern United States, they was found that there was a re-distribution of the zone of maximum cyclone frequency far to the south-west of normal. This was found to be linked to a strong ridge anomaly between Iceland and Greenland.

The Gyakum et al. (1996) study of cyclones during the Canadian Atlantic Storms Program II (CASP II; Stewart 1991) found results that were in partial agreement with the study of Dickson and Namais (1976). They contrasted the month of February 1990, in which only one explosive storm affected Atlantic Canada, and the month of February 1992, in which five explosive cyclones affected this region. It was found that February 1990 had an enhanced Icelandic Low, with a 30 hPa negative anomaly east of Iceland. That same month was characterised by a maximum warm anomaly of approximately 4.5°C over the Atlantic coastal region of the United States. February 1992 still had an enhanced Icelandic Low, but the maximum negative anomaly was weaker and shifted to the west of Iceland, with a strong cold anomaly near Baffin Island. This is suggestive that there indeed may be a link between the pressure over the Iceland-Greenland area, and the frequency of explosive development over coastal regions of eastern North America.

Lau (1988) also found a connection between the activity of the Atlantic “storm track” (as denoted by maxima in the root-mean-square bandpass (2.5-6 day) filtered geopotential height) and the 500-hPa circulation over the Atlantic Ocean. Moreover, he found that shifts in the “storm track” were related to distinctive patterns in this circulation. For example, when there was a prominent ridge over the Iceland area, with weakened upper-level flow in that region, the “storm track” had a nearly zonal orientation.

Various composite studies have documented the large-scale environment of explosive cyclones affecting eastern North America and the western Atlantic Ocean. Sanders and Davis (1988) studied thickness anomaly patterns associated with 67 cases of explosive cyclogenesis between 1962-1977. They found a strong cold anomaly centred over western Canada four days prior to the strongest explosive development. This anomaly moved south-eastward to lie just west of the eastern United States coast at the beginning of maximum deepening. A positive anomaly became evident over the Davis Strait two days before this time. They suggested that a necessary but not sufficient condition for extra intensity of a storm was a massive cold anomaly over North America, since the scale, coherence, and intensity of this cold anomaly was much less pronounced in cases of weak explosive development .

In a more recent paper, Lackmann et al. (1996) examined the planetary- and synoptic-scale characteristics of explosive cyclone development over the western Atlantic Ocean. They found a quasi-stationary ridge over western North America and two predecessor troughs that crossed the east coast of the continent prior to the onset of major deepening of cyclones in the western Atlantic. These troughs evolved out of north-westerly flow east of the stationary ridge, a finding consistent with Sanders (1988) study on the genesis of mobile upper troughs. An amplified planetary-scale wave pattern was also related to the temporal clustering of explosive cyclones, as opposed to isolated explosive events.

### 1.3 Thesis objectives

The above studies have looked primarily at the phenomenon of explosive cyclogenesis. They have revealed that the east coast of the United States and Atlantic Canada (New Brunswick, Nova Scotia, Prince Edward Island, Newfoundland) is a favoured area for these violent storms because of the presence of warm ocean currents and the cold conditions which prevail over the continent during the winter. There is also strong evidence that this phenomenon may have important connections to the large-scale environment, and that this environment can act to modulate and influence the positions of maximum explosive activity.

Links between the large-scale environment and the paths of individual weather systems tracking through or near Atlantic Canada will be examined in this study. The Atlantic provinces of Canada (Fig. 1.1) and their adjacent coastal waters are an area especially prone to severe storms. On average, an explosive cyclone will move through this region once a week in the winter (Stewart et al. 1995), although the numbers can vary considerably from year to year. In 1972 there were 35 storms on the east coast of Canada producing waves exceeding 6 m in height (Khandekar and Swail 1995). Linking the paths of cyclones to the large-scale environment would be of real value as a forecasting tool in this region and may yield insight as to the predictability of dangerous storms.

This study will not be limited only to cyclones that develop explosively. Though these cyclones are undoubtedly dangerous, deepening rate is just one measure of how dangerous a weather system may be. Anticyclones have also been known to cause high winds and considerable damage (Davis et al. 1993) and occasionally tropical cyclones and hurricanes cause devastation along the east coast. Wind speed will be used as a measure of which systems are studied, since it is high winds that are so dangerous to the marine community, and also to land-based populations. A similar technique was used by Davis et al. (1993) to develop a synoptic climatology of Atlantic coast 'northeasters'. They used as the basis of their study wave heights at Cape Hatteras producing at least 1.6 m deep-water waves.

Two stations, Halifax International Airport (44.5°N, 63.5°W) (hereafter we will simply refer to Halifax) and Sable Island (44°N, 60°W), will be used as point sources for

study purposes. It is recognised that by limiting the study to only these stations many dangerous weather systems may be missed. Over the ocean data are sparse, however, and the data at these stations allow us to gauge with continuity in time high wind activity in the region. Sable Island, though tiny and uninhabited, lies in the direct path of several principal storm tracks (Reitan 1974; Zishka and Smith 1980; Whittaker and Horn 1984), hence acquiring its nickname as “graveyard of the Atlantic”. Many ships sail near this rawinsonde station and over the years several have gone down with large loss of life. We have chosen Halifax for several reasons. It is the largest populated city in Atlantic Canada and lies on the eastern shore of Nova Scotia along which many cyclones track. As a port city, its year-round ice free harbour is of tremendous value. Also, owing to the small geographic area of the region, many of the weather systems affecting these stations would affect a large part of Atlantic Canada.

The current study will use hourly wind observations at Halifax and Sable Island as the basis of a study on high wind storms affecting Atlantic Canada between 1979-1995. The objectives are threefold:

- a) to provide a climatology of high wind storms for these stations and link anomalously active periods to large-scale circulation anomalies
- b) to examine the individual tracks and deepening rates of systems producing these winds
- c) to look for significant upper-level signatures several days prior to these wind storms.

If such signatures exist, and can be linked to the evolution of a high wind storm, then there exists the possibility of being able to use such signatures to improve the probability forecast of high wind storms.

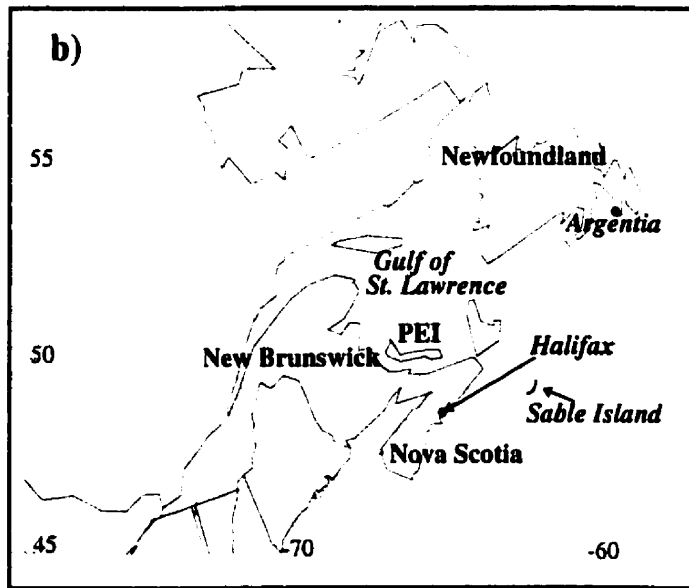


Fig. 1.1 Locator map for: a) North America, and b) Atlantic Canada.

## Chapter 2 - Data sets and analysis procedures

### 2.1 Data

The wind data used for this study were obtained from the archives of Canada's Atmospheric Environment Service (AES). Hourly measurements of wind speed and meteorological wind direction (to the nearest  $10^\circ$ ) were taken at level, open sites removed as much as possible from obstacles to wind flow. These were made by anemometers installed at 10 metres above the ground. Between 1985-1995 measurements were based on a two minute mean ending at the time of observation. Prior to 1985 a one minute mean was used. This represents a limitation in comparing results before and after 1985 since there could be a reduction in the amplitude of maximum sustained winds beyond 1984 due to increased smoothing from a two minute mean. However, a clear bias towards higher wind speeds before 1985 is not evident, since the year with the highest number of high wind storms at Sable Island occurred in 1988. Additionally, some of the highest wind speed values in our data occurred between 1985-1995.

Hourly data of both wind speed and direction were analysed for the period 1979-1995 at Halifax and Sable Island. Since there were missing data after 1991, data were filled in by linear interpolation between the vector components of the wind data immediately preceding and following the missing hourly observations. Data were rarely missing for more than six hours on any given day. In our search for the highest wind speeds during the period of study this may skew the results toward the period before 1992.

All gridded data used were taken from the National Centers for Environmental Prediction (NCEP) reanalyses data set (Kalnay et al. 1996), which has a horizontal resolution of  $2.5^\circ$  latitude by  $2.5^\circ$  longitude. The NCEP reanalyses project uses a frozen data assimilation system and was designed to remedy the problem of climate drift brought about by changes in forecast and analysis procedures over the years. Although data from this project is now available from 1957 to the present, we use data for the years 1979-1995 since that is what was available at the time of this study. For a relevant discussion



on comparisons between the NCEP reanalyses and other sets of data the reader can refer to Betts et al. (1996), Basist and Chelliah (1997), Mo and Higgins (1996) or Gutowski et al. (1997). This study will utilise 1000- and 500-hPa geopotential height and sea-level pressure (hereafter SLP) fields at a temporal resolution of 6 hours (0000, 0600, 1200, and 1800 UTC). Because we are using what is termed by Kalnay et al. (1996) as type A data (meaning the analysis variable is strongly influenced by observed data and is hence most reliable), it is believed that this is a useful data set for the purposes of this study since it incorporates many sources of observations not available in real time for operational analyses. All gridded fields were input into the General Meteorological Package (GEMPAK) (desJardins et al. 1991) for viewing purposes and for the tracking of cyclone centres.

## **2.2 Analysis of wind data**

In this study, a high wind event (hereafter HWE) at Halifax will be required to have a wind speed value of at least  $15 \text{ m s}^{-1}$ , while at Sable Island a HWE will be required to have a wind speed value of at least  $20 \text{ m s}^{-1}$ . At both stations, these values occur in the lowest percentile of all wind speed observations (Table 2.1). The lower minimum threshold for a HWE at Halifax is because of its land-based location where frictional effects will be more important in slowing the wind than at Sable Island.

By comparison, inland high wind warnings are issued to Atlantic Canada by Environment Canada when sustained winds are forecast to reach values of  $18 \text{ m s}^{-1}$  or gusts to reach  $25 \text{ m s}^{-1}$  during the short-term forecast period. The marine community is issued a wind warning if forecast winds are to reach  $25 \text{ m s}^{-1}$  during the short-term period.

A search was performed at both Halifax and Sable Island for the highest wind speed in each consecutive 48 hour period starting at 0:00 Atlantic Standard Time (0400 UTC). We identified all those wind speed values which satisfied the specified threshold criteria and labelled them a high wind event (hereafter HWE). In the event that two adjacent 48 hour periods contained wind speeds which met the criteria but which were

separated by less than 48 hours, only the highest value was retained and selected as a HWE.

Table 2.1 Percent occurrence of hourly wind speeds for 1979-1995.

Wind speed ( $s$ ) ( $\text{m s}^{-1}$ )	occurrence (%) - Halifax	occurrence (%) - Sable Island
$0 \leq s < 5$	57.47	34.33
$5 \leq s < 10$	39.56	46.85
$10 \leq s < 15$	2.84	15.80
$15 \leq s < 20$	0.13	2.75
$20 \leq s < 25$	0.005	0.25
$25 \leq s < 30$	-	0.02
$30 \leq s < 35$	-	0.0004

For the purposes of this study, we will classify each high wind event according to the quadrant into which its wind direction falls—i.e., meteorological wind direction in one of four groups:  $1^\circ - 90^\circ$  (hereafter NE),  $91^\circ - 180^\circ$  (hereafter SE),  $181^\circ - 270^\circ$  (hereafter SW),  $271^\circ - 360^\circ$  (hereafter NW). Owing to Nova Scotia's south-west to north-east alignment and Halifax's position on the eastern shore of Nova Scotia, one might expect that low-level winds coming off the land (i.e., possessing a northerly component) would be significantly reduced due to friction. This effect would be much less pronounced at Sable Island, which is essentially a tiny sandbar located in the Atlantic Ocean about 300 km east of Halifax. There is also incentive to study HWEs categorised by wind direction since direction would be indicative of a weather system's position relative to our stations and imply differences in tracks and synoptic-scale environments.

### 2.3 Composite methodology

We define for this study H+00 as the nearest six hourly value in UTC (i.e. 0000, 0600, 1200, 1800 UTC) to the hour of the peak wind speed observation at our stations. If the hour of the peak wind observation fell on the midpoint between these six hourly values, it was taken to the higher six hourly value (e.g., peak wind value at 0300 UTC would be designated H+00 at 0600 UTC). The composite procedure was used to identify

the synoptic-scale environment associated with HWEs classified by wind quadrant. This was done for both Halifax and Sable Island and results reveal distinct differences between the two stations. However, because of the higher number and intensity of HWEs at Sable Island (see Table 3.1) we will limit our composite discussions to that station.

One inherent difficulty with a composite field is that it is a smoothed version of the individual fields from which it is derived. The scales and intensity of features within a composite may not be representative of the majority of the individual cases from which it is derived since a single anomalous case can skew the resultant composite. To address this difficulty, a two-sided Student's t-test was applied to each composite field (see Panofsky and Brier 1968, section 3.4) to test its significance.

#### **2.4 Linear correlation analysis**

Although the Student's t-test gives a test of significance to each composite field it is still desirable to remove those fields whose features skew the results, in order to obtain a composite field which is as representative as possible of the "typical" environment of a HWE (we are interested in extreme cases, of course, but these are not generic and need to be addressed in individual case studies). To address this issue, we followed the clustering technique of Lund (1963). This categorises gridded fields in the following manner:

- 1) Each gridded field is linearly correlated with every other field and the correlation coefficient matrix computed.
- 2) That field with the most correlation coefficients assigned to it at or above a threshold value of 0.6 is removed and called field A.
- 3) Remove all fields correlated with field A at or above the threshold value. Call these fields together with field A group A. Select from those remaining the field with the most correlation coefficients meeting the threshold criteria and call it field B.
- 4) Repeat this procedure until only a few cases remain which are correlated to one another at the threshold value.

This procedure is sensitive to the time and fields on which it is performed. Lund (1963) used SLP maps and prescribed a correlation coefficient threshold value of 0.7. Stoss and Mullen (1995) correlated 500-hPa anomaly fields and used a threshold of 0.5. Because we are most interested in a typical flow configuration at the time of a HWE, H+00 is chosen as the time at which to perform the clustering technique.

Experiments were performed on the sensitivity of the groups to correlation between anomaly fields and raw fields, as well as sensitivity to the parameter (i.e. 1000-hPa vs. 500-hPa heights). It was found that it was easier to obtain high correlation by correlating raw geopotential height fields than by correlating geopotential height anomaly fields. Higher correlation was also obtained when correlating at the 500 hPa level. This is no surprise since there is more variability in surface fields and since climatological features (such as the Icelandic surface low) would have less variance on a temporal basis and give higher field to field correlation when using raw fields. To be as stringent as possible, and since it is strong gradients in the surface mass fields which are responsible for the high winds, we choose to correlate 1000-hPa anomaly fields. We are interested in anomalies, but it is recognised that they possess a limitation since they are sensitive to the climatology from which they are derived. All anomalies were calculated as departures from the monthly weighted average climatology from 1979-1995. A correlation threshold of 0.6 was chosen since this is a slightly higher value than that employed by Stoss and Mullen (1995) on their anomaly fields and since it is a fairly stringent number to use on a surface anomaly field.

One other limitation should also be noted. The results of the linear correlation analysis are sensitive to the region of the grid on which the calculations are performed. This question will be addressed in chapter 4.

## **2.5 Cyclone tracks**

Despite the above statistical measures, there is still the question as to the reality of composite cyclone tracks. To address this point, we tracked surface cyclone centres from H-96 to H+36. This was accomplished in the following manner. The nearest pressure

minimum giving cyclonic flow to Sable Island at H+00 was identified and designated for tracking. It is important to realise that in some cases high winds occurred in anticyclonic flow, in which case there was no cyclone designated for tracking. This pressure minimum was tracked backwards in time in six hour increments until it could no longer be found at a contour interval of 2 hPa or until H-96 was reached—whichever came first. The pressure minimum was tracked forward in time from H+00 to H+36 or until the cyclone centre disappeared or lost its identity in a larger-scale pre-existing cyclone—whichever came first. All tracks were derived from the NCEP reanalyses sea level pressure grids viewed in GEMPAK.

It is recognised that these tracks and the associated central SLP values of cyclones are not completely accurate since the fields are a blend of forecast model output and observations at a resolution which cannot hope to completely resolve individual mesoscale features. However, for the purposes of this study, we are interested only in the general features of surface cyclone tracks and in comparing them with composite tracks. The greatest difficulty with this method is in our discussion of rapid deepening, since there are often large differences between the lowest observed central pressure of a cyclone and that of the analysis (Gyakum 1983a). We can say, however, that our deepening rates will generally be *underestimated*.

## Chapter 3 - Climatology of high wind events for the period 1979-1995

### 3.1 Interannual and monthly variability of high wind events

Sable Island typically experiences more HWEs than Halifax, with annual numbers varying from a low of three in 1995 to 12 in 1988 (Fig. 3.1). At Halifax there were no HWEs in 1991, with a peak of 10 in 1983. Both stations experienced a sharp decline in the number of events between 1984-1986. Despite their relative proximity, it is also evident from Fig. 3.1 that high winds from a given weather system often do not affect both stations. This is especially evident during the period 1986-1988.

A large number of HWEs in a year may be the result of several windstorms spread throughout the year, or the result of a single active month (Fig. 3.3). Six of the 11 HWEs at Sable Island in 1982 occurred during the month of January (to be discussed in section 3.2). By contrast, the 12 events in 1988 at Sable Island were the result of active months at both the beginning and end of the year (Fig. 3.3).

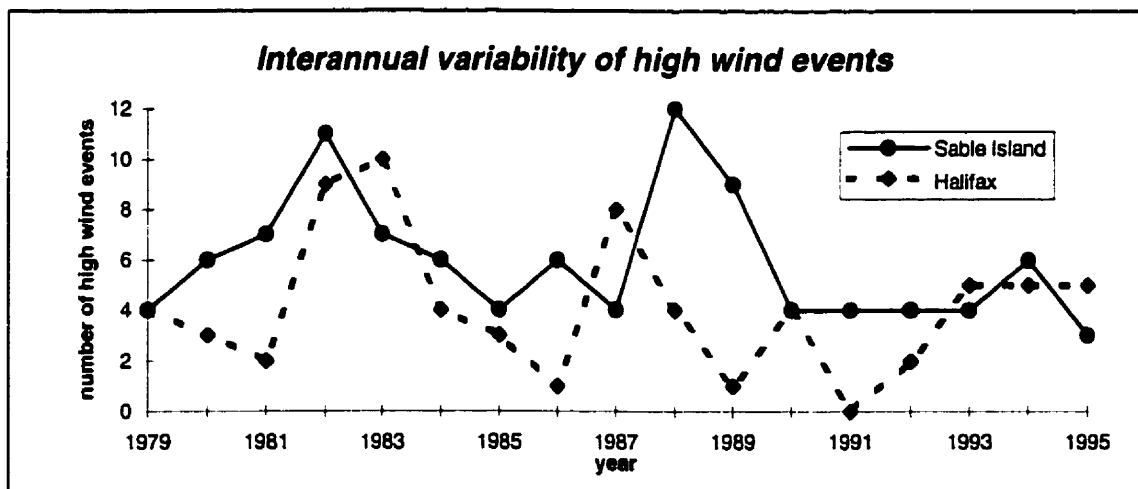


Fig. 3.1 Number of high wind events each year giving winds over  $20 \text{ m s}^{-1}$  at Sable Island (solid) and giving winds over  $15 \text{ m s}^{-1}$  at Halifax (dashed).

The seasonal distribution of HWEs shows a maximum in winter months, peaking in January, and a pronounced minimum in summer months (Fig. 3.2). This is not surprising, since there is a significant reduction in the magnitude of the thermal wind in

mid-latitudes during the Northern Hemisphere warm season when overall baroclinicity is weak relative to winter months. Several studies (e.g., Roebber 1984; Zishka and Smith 1980; Reitan 1974) have shown that related to this is a sharp decline in the number of cyclones during the warm season along the east coast<sup>1</sup>. It is significant that more HWEs occur in November at both Halifax and Sable Island than either February or March. If we were to define a HWE season as the number of consecutive months containing 5% of all HWEs, then the season at both stations would extend for six months, from November through April.

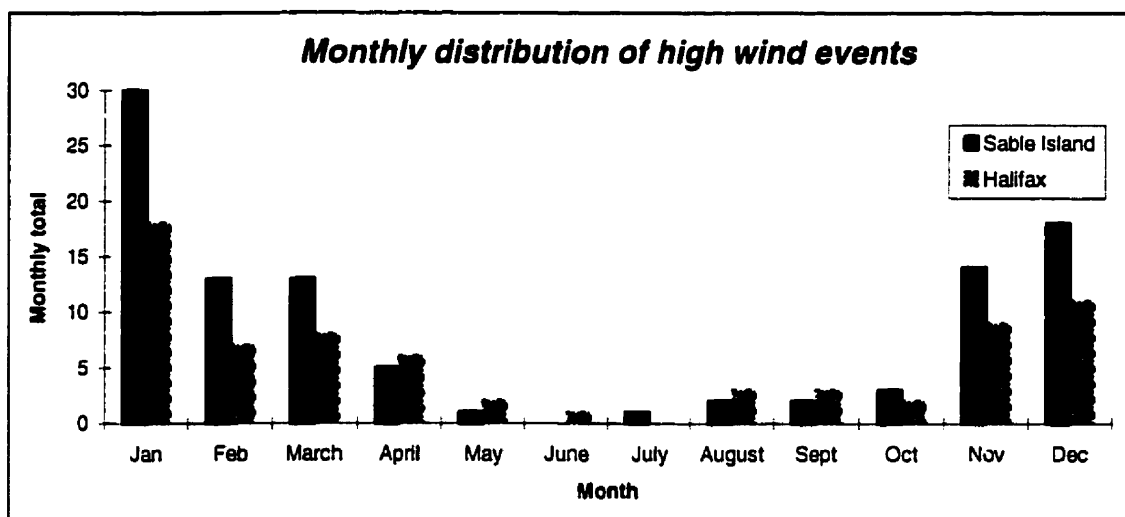


Fig. 3.2 Monthly distribution of high wind events (1979-1995).

The Uccellini and Kocin (1990) study of snowstorms along the northeastern coast of the United States documented the physical and dynamical processes associated with several of the most crippling snowstorms to affect the north-eastern United States. The time of overlap between their study and this one—1979-1987—revealed that four out of the six snowstorms they studied during this period corresponded to a HWE at Sable Island. This emphasises the importance of our study for regions other than the Atlantic Provinces of Canada.

<sup>1</sup> Despite the rarity of HWEs in summer months, there is no guarantee that they will be less severe. The *Queen Elizabeth II* storm (Gyakum 1983a,b) was the most rapidly deepening storm in the Sanders and Gyakum (1980) study on “bombs”. This was a baroclinic disturbance giving hurricane force winds that occurred 10-11 September 1978 and attained a central pressure estimated at 945 hPa.

### 3.2 The contrasting periods of January 1982 and January 1984

One objective of this study is to find a relationship between the large-scale circulation and periods with unusually high numbers of HWEs at Halifax and Sable Island. As a rudimentary attempt to determine this relationship, two months with contrasting numbers of HWEs were examined, January 1982 and January 1984 (Fig. 3.3). To relate these anomalous periods to the large-scale flow, composites of 1000-500 hPa thickness, 500-hPa geopotential height, and SLP were generated. Anomalies were calculated as the difference of the composite value at each grid point from the January climatological mean for the period 1979-1995.

#### *a) January 1982*

January 1982 was an exceptionally stormy month over Atlantic Canada. The six HWEs which occurred at Sable Island represented at least twice the number found in any other month during our period of study. There were only short periods of relative calm at both stations (Fig 3.4) and only once during the month did winds remain below  $10 \text{ m s}^{-1}$  at Sable Island for more than two days. Some periods, as on the 18<sup>th</sup> and 19<sup>th</sup>, were characterised by prolonged sustained winds, while other high wind activity lasted only a few hours—as on the 10<sup>th</sup> and 27<sup>th</sup> at Sable Island. The high winds occurring on the 16<sup>th</sup> were related to a cyclone so severe that schools throughout the Maritimes had to be closed for 4 days due to heavy snowfall and bitter cold. The cold surge that followed broke the all time record low at Charlottetown ( $-30.4^\circ \text{C}$ ) (obtained from the Atmospheric Environment Service *Climate Perspectives* 1982).

Strong zonal flow prevailed over the North American continent in January 1982 as a deep Arctic air mass affected much of Canada and the United States (Figs. 3.5-3.6). This feature resulted from blocking activity related to a strong ridge over the Beaufort Sea and brought persistent cold over much of Canada throughout the month. Wagner (1982) reported the central and northeast United States endured record breaking cold surges during January 1982, although the cold was tempered by brief mild spells. These



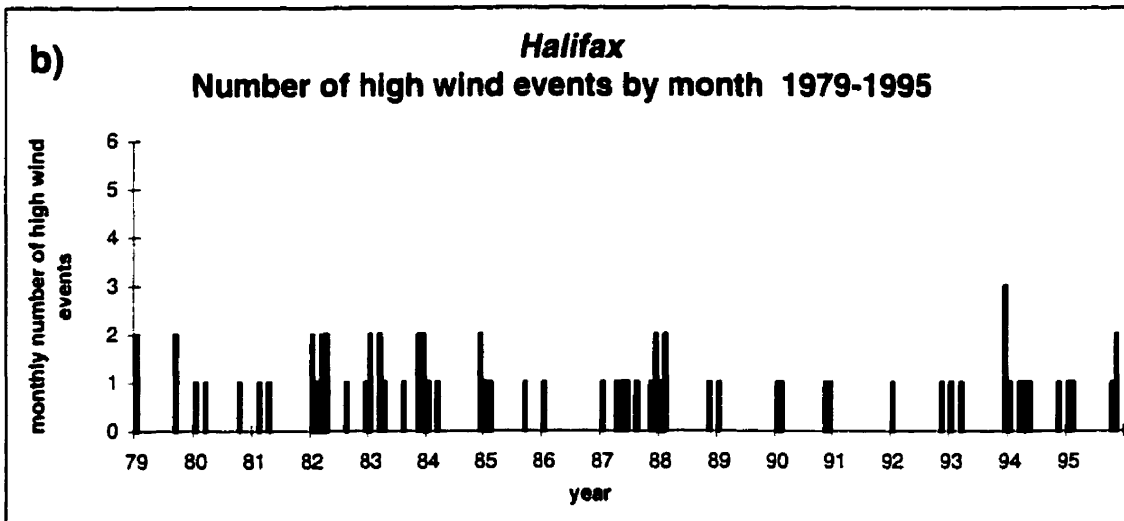
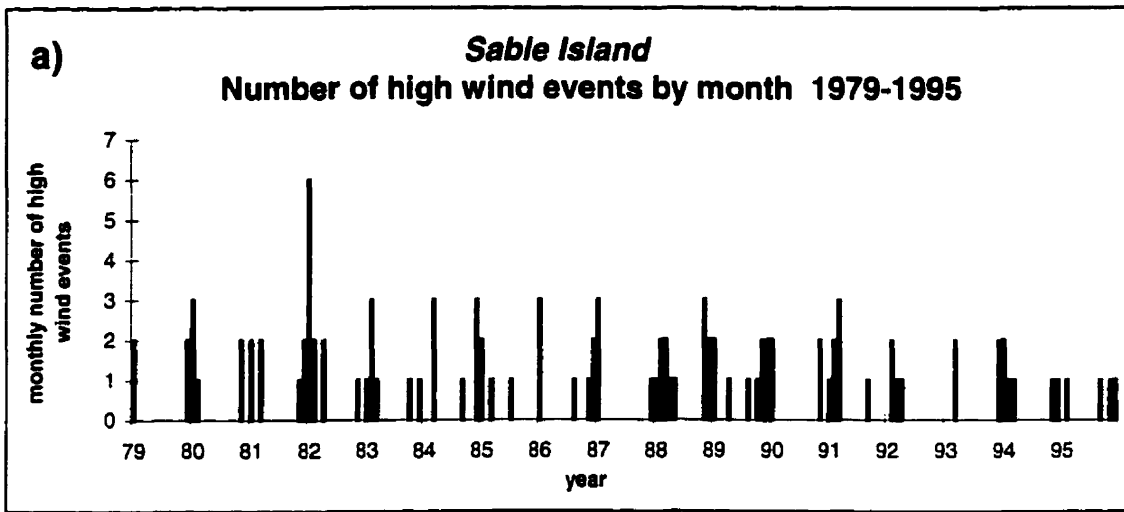


Fig. 3.3 Total number of high wind events each month at: a) Sable Island and b) Halifax.

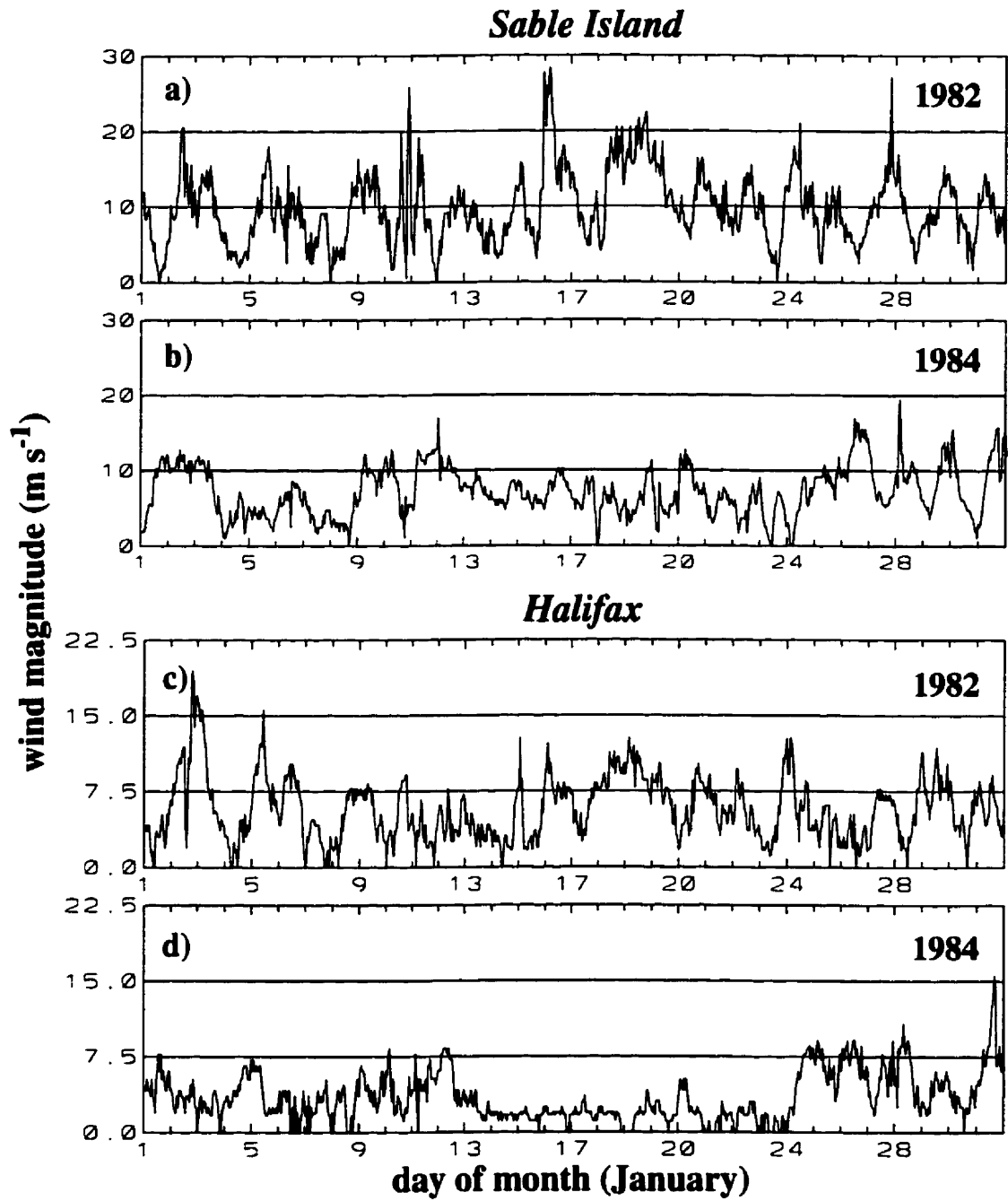


Fig. 3.4 Time series of wind speed for a) Sable Island (January 1982), b) Sable Island (January 1984), c) Halifax (January 1982), and d) Halifax (January 1984). Values of wind speed are in m s<sup>-1</sup>.

conditions would have greatly enhanced the coastal baroclinicity as cold Arctic air was in close proximity to warm maritime air along the east coast. Intense cold air outbreaks were found by Konrad and Colucci (1989) to precede strong surface cyclogenesis over eastern North America. Their second most intense cold air outbreak occurred on 10 January 1982, and was associated with a cyclone with a deepening rate of 2.5 bergerons giving sustained winds of  $25 \text{ m s}^{-1}$  to Sable Island (Fig. 3.4). The same storm gave the second highest storm surge of this century to Argentia, on the western shore of the Avalon peninsula, Newfoundland (Murty et al. 1995).

A second important feature in Figs. 3.5-3.6 is the circulation over the Atlantic Ocean. The climatological Icelandic Low is weaker than normal, while there is a pronounced negative anomaly in the central North Atlantic near  $45^\circ \text{ N}$ ,  $30^\circ \text{ W}$ . This Atlantic pattern resembles the negative phase of the North Atlantic Oscillation (NAO) as found by Rogers (1990), who associated this with a maximum in cyclone frequency over Atlantic Canada. It is suggestive that during this Atlantic pattern there is a preference for storms to track through the Atlantic Canada region.

#### *b) January 1984*

January 1984 was an unusually calm period (Fig. 3.4) in contrast to January 1982. There is evidence from the wind speed trace at both stations that the atmospheric state during the middle of the month was quite different from the rest of the month. This is especially evident at Halifax, where the winds only exceeded  $5 \text{ m s}^{-1}$  once in the period from the 13<sup>th</sup> to the 24<sup>th</sup>. This calm period corresponded with bitter cold over much of eastern North America (Quiroz 1984). Only one HWE occurred at Halifax on 31 January while there was no event for the month at Sable Island.

An unusually deep Icelandic Low and a strong, nearly barotropic ridge anomaly extended zonally across the central North Atlantic (Fig. 3.6) during this month. This was related to a strong upper tropospheric jet at  $50\text{-}60^\circ \text{ N}$  over the Atlantic Ocean which was the strongest jet-level wind anomaly of the winter (Quiroz 1984). There was also a stronger mean north-south flow component than January 1982 related to a large-

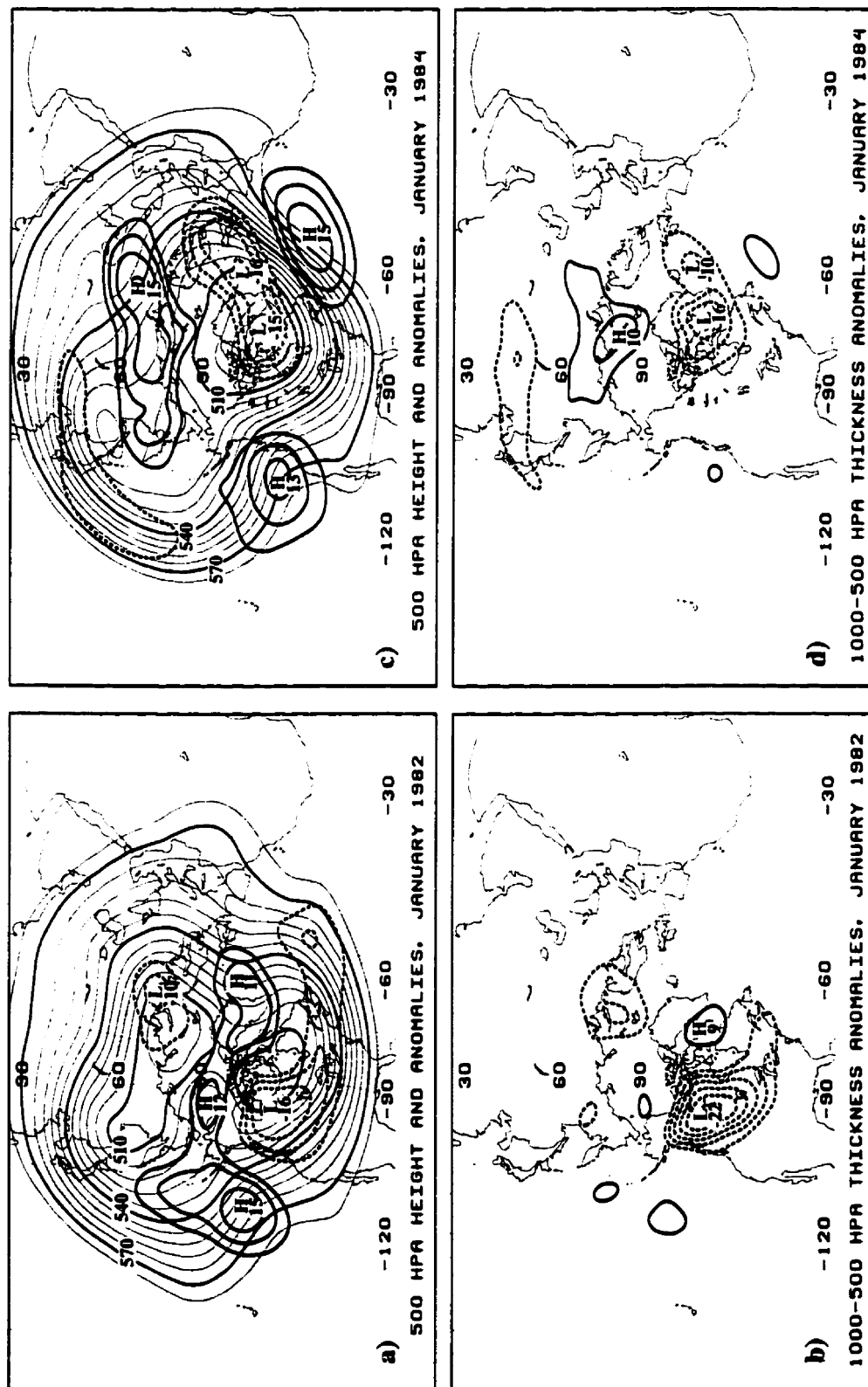


Fig. 3.5. Composite 500-hPa geopotential height (every 6 dam, panels a) and c)), geopotential height anomalies (panels a) and c)), and 1000-500 hPa thickness anomalies (panels b) and d)). Positive (negative) anomalies are solid (dashed) every 3 dam. The 0 and 3 (-3) positive (negative) contours are omitted for clarity. Panels a)-b) are for January 1982 and panels c)-d) are for January 1984.

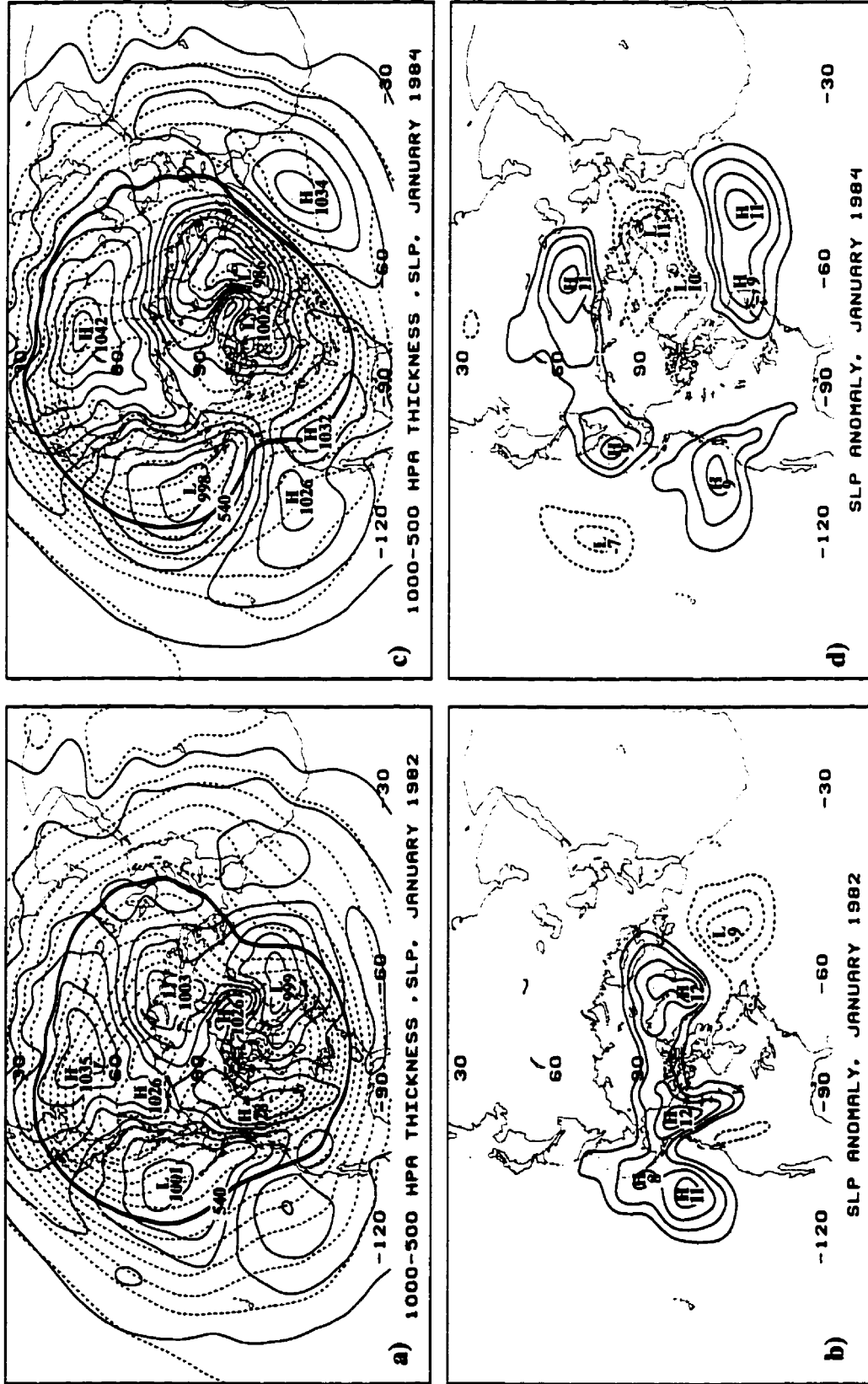


Fig. 3.6. Composite 1000-500 hPa thickness (dashed, every 6 dam, with 540 hPa thickness in heavy solid) and sea-level pressure (solid, every 4 hPa) in panels a) and c). Sea-level pressure anomalies [positive (negative) contours are solid (dashed)] every 2 hPa with the 0 and 3 (-3) positive (negative) contours omitted for clarity are in panels b) and d). Composites are for January 1982 in panels a)-b) and for January 1984 in panels c)-d).

amplitude trough centred over the North American continent. This suggests that an enhanced Atlantic jet associated with a deepening of the climatological Icelandic Low may be an important factor in inhibiting HWEs over Atlantic Canada. However, it cannot be said to inhibit cyclogenesis, since there may simply be a shift in the region of main cyclone activity to the north of the Atlantic Provinces. Caution, however, must be exercised, since January 1984 was characterised by alternating atmospheric states. The first and last weeks of the month were warmer than usual over eastern North America, while a strong blocking event near Alaska during 8-21 January brought extreme cold to Canada and the eastern USA (Quiroz 1984).

Severe cold over much of eastern Canada was a characteristic common to both months and may have played a strong role in the high number of storms in January 1982. Yet in the period of severe cold for January 1984 winds were generally quite weak with no HWEs. This raises the question as to why there was such a difference between the two months. The answer may be related to the circulation over the Atlantic Ocean, which was very different for these two periods. One condition for high numbers of HWEs over Halifax and Sable Island may be a weakening of the climatological Icelandic Low and the upper-level circulation over the central Atlantic.

### **3.3 Categorising high wind events by wind direction**

Table 3.1 gives a categorisation of HWEs at both stations according to their wind direction. There were no NE HWEs at Halifax, with the maximum northeast wind speed almost  $5 \text{ m s}^{-1}$  less than the maximum wind speed in the other quadrants. To the general public this might come as a surprise, since stormy weather is often associated with the famed 'northeaster'. This perception has a basis, since northeast winds occur in a sector of cyclones typically characterised by a long history of ascent and an abundance of moisture. When combined with cold northern air this often leads to large snowfalls (Uccellini and Kocin 1987).

There were a high number of HWEs in the SW quadrant at both stations. While the most HWEs at Halifax occurred in the SE quadrant, at Sable Island this quadrant possesses the fewest number of events.

Two well known storms gave peak winds at both stations. The "Halloween" storm of 28-31 October 1991 (Davis and Dolan 1992) gave the highest northeast winds at both Halifax and Sable Island during our period of study. The Ocean Ranger storm of 12-14 February 1982 (Kuo et al. 1991) gave the highest sustained winds ( $30.8 \text{ m s}^{-1}$ ) at Sable Island.

**Table 3.1 Total number of high wind events and peak wind speed in each wind quadrant.**

Direction	Halifax		Sable Island	
	Total	Maximum ( $\text{m s}^{-1}$ )	Total	Maximum ( $\text{m s}^{-1}$ )
NE	0	14.4	22	25.8
SE	29	21.7	19	27.2
SW	28	19.2	33	28.9
NW	13	19.4	28	30.8

*a) Frictional and gradient wind effects*

The gradient wind effect may explain why there were no HWEs in the NE quadrant at Halifax. The trajectory curvature in that quadrant would be significantly cyclonic for northeastward moving cyclones and the wind speed noticeably weaker than its geostrophic value. Friction from the overland northerly component of the wind would additionally slow the wind. The combined effects would give a possible explanation for the lack of HWEs in that quadrant for Halifax. At Sable Island, the gradient wind effect would account for the relatively small number of HWEs in that quadrant. However, the high number relative to Halifax might be due to reduced friction owing to its marine location.

The most important reason for the high numbers in the SE quadrant at Halifax is that southeast wind flow is directly off the Atlantic Ocean and frictional effects would be minimised relative to other directions.

The high numbers in the SW quadrant at both stations may also be explained by the gradient wind effect. For northeastward moving cyclones we generally expect centrifugal forces to be the least important in this quadrant, and the wind speed to be closest to its geostrophic value.

Weinstein and Sanders (1989) stated that within the naval community “a common query regards the strongest wind” in a rapidly intensifying cyclone. They studied cases of rapidly deepening cyclones in the North Atlantic Ocean to determine a relationship between geostrophic wind and pressure fall. Observed wind was not used to derive a relationship between pressure fall and wind speed since observed winds are sparse over the ocean. With the available data they found that the maximum observed wind anywhere in the cyclone tended to be in the southeast and southwest quadrants, with a distinct minimum in the northwest quadrant where centrifugal forces are important. An important distinction to be made is that their quadrants are not based on the meteorological wind direction, but rather on the quadrant of a cyclone relative to a Cartesian co-ordinate system. Hence, their maximum in the southeast and southwest quadrant would correspond to approximately our SW and NW quadrants respectively (of course ageostrophic effects will change the direction of the observed wind somewhat so that, for instance, a northeast wind may not fall in the northwest quadrant of the cyclone). Because we are looking at a fixed location, it is difficult to draw comparisons to their study. However, it is significant to find at Sable Island agreement with their finding that maximum wind strength appears to be from the southwest and northwest direction.

Weinstein and Sanders (1989) also found that the maximum wind was rarely found in the northwest sector of a cyclone and suggested the gradient wind effect as a possible explanation. This is in agreement with our finding that the maximum wind speed in the NE quadrant was the weakest of all four quadrants and that there were comparatively few NE HWEs in comparison to the SW and NW quadrants.

#### *b) Selection of HWEs affecting Sable Island for further study*

Because of the strength and high number of HWEs at Sable Island and the danger they pose to the marine community, these weather systems are examined in more detail.



Although storms affecting Halifax are important, this study will focus further on Sable Island since the potential threat to human life at sea is greater for systems affecting that station.

To give equal weight to each wind quadrant, the date and hour of the 30 highest wind observations in each quadrant at Sable Island from the period 1979-1995 were selected for further study. If a date fell in more than one quadrant, only that date with the highest wind speed was retained. This was done to retain the independence of all 120 cases and facilitate inter-quadrant comparisons. One limitation of this method is that sometimes the same date occurred in both the NE and NW quadrants. Since northeast winds were generally weaker it was occasionally necessary to discard the northeast wind and choose another weaker northeast observation for further study. Statistics are given on case selections in Table 3.2. In order to obtain 30 events in each wind quadrant, some cases were taken which did not explicitly meet the minimum value required for a HWE. However, for simplicity these will still be referred to as HWEs since the minimum value was still a respectable  $18.6 \text{ m s}^{-1}$ .

**Table 3.2 Statistics for 30 selected cases in each wind quadrant at Sable Island**

Quadrant	Average speed ( $\text{m s}^{-1}$ )	Standard deviation ( $\text{m s}^{-1}$ )	Minimum ( $\text{m s}^{-1}$ )	maximum ( $\text{m s}^{-1}$ )
NE	21.0	1.7	18.6	25.8
SE	21.0	2.0	19.2	27.2
SW	23.4	2.4	20.6	28.9
NW	22.6	2.4	19.2	30.8

*c) The persistence parameter*

As a check on the validity of classifying HWEs according to their wind direction, the persistence of the wind over a 24 hour interval was computed in a manner similar to Panofsky and Brier (1968). It is defined as

$$\text{Persistence} = \frac{W_r}{W_m} \quad (3.1)$$

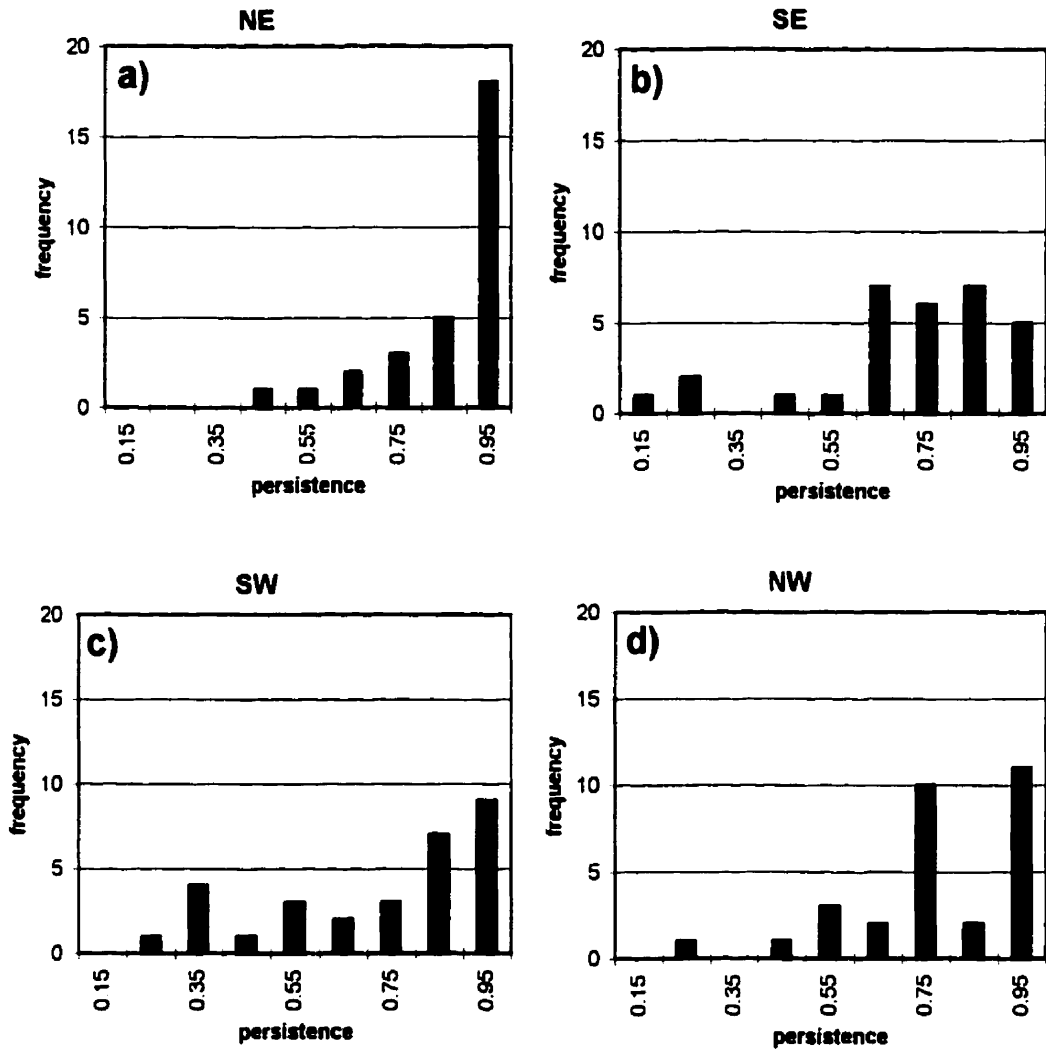


Fig. 3.7 Persistence frequency for top 30 HWEs at Sable Island for: a) the NE quadrant, b) the SE quadrant, c) the SW quadrant, and d) the NW quadrant. Persistence values are calculated over the period from 12 hours preceding the peak wind speed to 11 hours following the peak wind speed.

where

$$W_r = \sqrt{R_x^2 + R_y^2}, \quad (3.2)$$

$$W_m = \frac{1}{N} \sum_{i=1}^N |\bar{u}_i|, \quad (3.3)$$

and

$$R_x = -\frac{1}{N} \sum_{i=1}^N |\bar{u}_i| \sin \theta_i \quad (3.4)$$

$$R_y = -\frac{1}{N} \sum_{i=1}^N |\bar{u}_i| \cos \theta_i \quad (3.5)$$

Here,  $N$  is the number of observations which is taken to be 24--from 12 hours before the peak wind speed observation to 11 hours following the peak wind speed observation. As well,  $|\bar{u}_i|$  is the magnitude of the hourly wind, and  $\theta_i$  is the meteorological wind direction. Persistence is simply the ratio of the resultant wind to the mean wind over a given period and a measure of how persistent the wind was in a given direction over that time interval. A value of 1.00 would mean the wind direction was unchanging while a value of zero would imply opposite wind directions for equal amounts of time. The direction of the resultant wind also gives information as to what the dominant direction over the period is. This is useful, since a HWE may be due to the passage of a front and a sudden shift in wind direction that is not representative of the period. A high persistence with a resultant wind in a quadrant different from that of the maximum observation would imply a shift in the wind direction near the end of the 24 hour interval and would suggest classifying that HWE in a different wind quadrant. A low persistence would imply that the peak in wind might have been due to the passage of a front. The resultant wind direction rarely fell in a quadrant that was different from that of a HWE.

The NE quadrant, despite the relative weakness of its maximum winds, is characterised by high persistence at Sable Island, with 18 out of 30 cases having a value greater than 0.9 (Fig. 3.7). A possible explanation for this is that the weather systems

producing these winds move slowly. Cyclone tracking results in the next chapter confirm this, with phase velocities generally being lowest in this quadrant.

In general, however, there are very few cases with persistence less than 0.5 (Fig. 3.7) and this gives a degree of confidence in dealing with each quadrant separately.

#### *d) Duration of high winds*

Important differences are evident when the evolution of winds at Sable Island in a 24 hour period bracketing the peak wind observation are examined. Figure 3.8 gives the time series of wind speed averaged by wind quadrant among all cases up to and including 1991. Excluded from this average were all dates after 1991, since several hours of data were missing. This means that the average included 24, 25, 26, and 22 cases for the NE, SE, SW, and NW quadrants respectively.

In general, the NW quadrant appears to be the most dangerous, with winds on average maintaining velocities exceeding  $15 \text{ m s}^{-1}$  for 12-15 hours. This is consistent with Khandekar and Swail's (1995) finding that peak significant wave heights (defined to be the average of the top third of all wave heights) usually occur in northwesterly flow behind ocean cyclones. The high standard deviation in the NW quadrant in the 12 hours preceding the HWE indicates a high degree of variability in these weather systems during that time. Continental versus oceanic storm tracks are partly responsible, as evidenced in the paths of many of these cyclones (discussed in chapter 4, see Fig. 4.9). However, in the hours following the peak winds, the standard deviation is greatly reduced, while the winds remain relatively strong. Another interesting feature is the sharp increase in wind magnitude from two hours before the peak observation to its maximum value (also evident in the SW quadrant).

In contrast to the NW quadrant, the standard deviation in the 12 hours preceding the peak wind observation in the SE quadrant is much smaller, with a nearly constant rise in wind speed from a very low value at H-12. After its maximum value, there is a sharp decline in wind velocity, while the standard deviation nearly doubles six hours later. The

reason for this increase in standard deviation is not clear, though an obvious possibility is differences in the phase velocities of these systems. This is the least dangerous of the quadrants, with wind velocity exceeding  $15 \text{ m s}^{-1}$  for only 2-4 hours on average.

There has been evidence through examining persistence that systems giving strong northeast winds to Sable Island move slowly. They also tend to give weak maximum winds relative to other quadrants. However, evidence from Fig. 3.8 shows that on average our NE systems give sustained winds exceeding  $15 \text{ m s}^{-1}$  for 12-14 hours. The slow phase velocity of these systems, high values of persistence, and evidence that they often stall to the east of Sable Island (to be shown in chapter 4) support this finding. The duration of these HWEs (at least in some cases) suggests that although the peak winds from NE systems are not usually strong, they can still be considered dangerous.

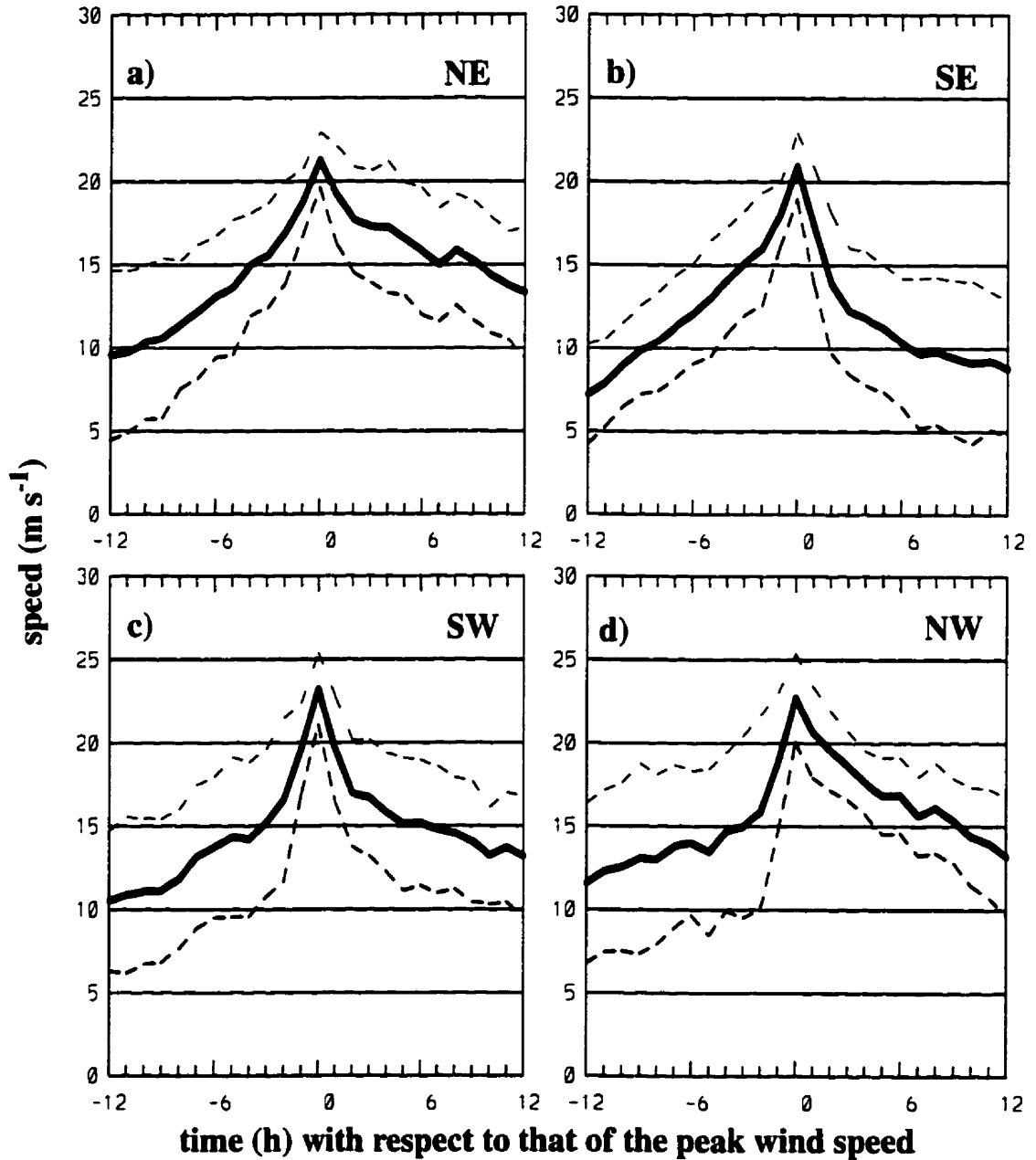


Fig. 3.8. Average wind speed (heavy solid;  $\text{m s}^{-1}$ ), average wind speed plus one standard deviation (upper dashed;  $\text{m s}^{-1}$ ), and average wind speed minus one standard deviation (lower dashed;  $\text{m s}^{-1}$ ) for each wind quadrant. The average represents all dates from 1979-1991 for the: a) NE quadrant, b) SE quadrant, c) SW quadrant, d) NW quadrant.

## **4. Planetary- and synoptic-scale structure associated with high wind events at Sable Island**

### **4.1 Introduction**

A number of studies (e.g., Sanders and Gyakum 1980; Sanders 1986; Manobianco 1989) have shown that a critical forcing mechanism for explosive cyclogenesis is the presence of an upstream upper-level trough. This is in agreement with theoretical studies using linear stability analysis to find regions of preferred instability (e.g., Frederikson 1979a). Other studies, such as Lackmann et al. (1996), have shown the development of a 500-hPa ridge downstream from the cyclogenetic trough as rapid development occurs and suggested that diabatic effects such as latent heat release are important in amplifying the ridge often seen ahead of strong coastal cyclones. These studies imply that a favourable region for a correlation analysis (discussed in chapter 2) would be that associated with an upper-level trough-ridge couplet, as opposed to just an upper-level trough.

We have chosen to correlate 1000-hPa height anomalies at H+00 since high winds are due largely to strong gradients in the surface mass fields. The assumption is made that the nearest 500-hPa trough-ridge couplet to Sable Island (as denoted by the geopotential height anomaly fields at that level) is having a direct influence on surface pressure gradients. The composite 500-hPa geopotential height and anomaly fields at H+00 associated with the top 30 cases in each wind quadrant were obtained (Fig. 4.1). A linear correlation analysis was then performed within the region enclosing the nearest trough or trough-ridge couplet to Sable Island. The regions are outlined in bold in Fig. 4.1, and the numbers associated with each group found are given in Table 4.1. Anomalies within the four regions are all statistically significant at 95% or above according to a Students t-test. Because there was one prominent group of over 20 cases in the NE, SE, and NW quadrant, we will present only the results based on these groups. For the SW quadrant we will present the results based on the two largest groups.

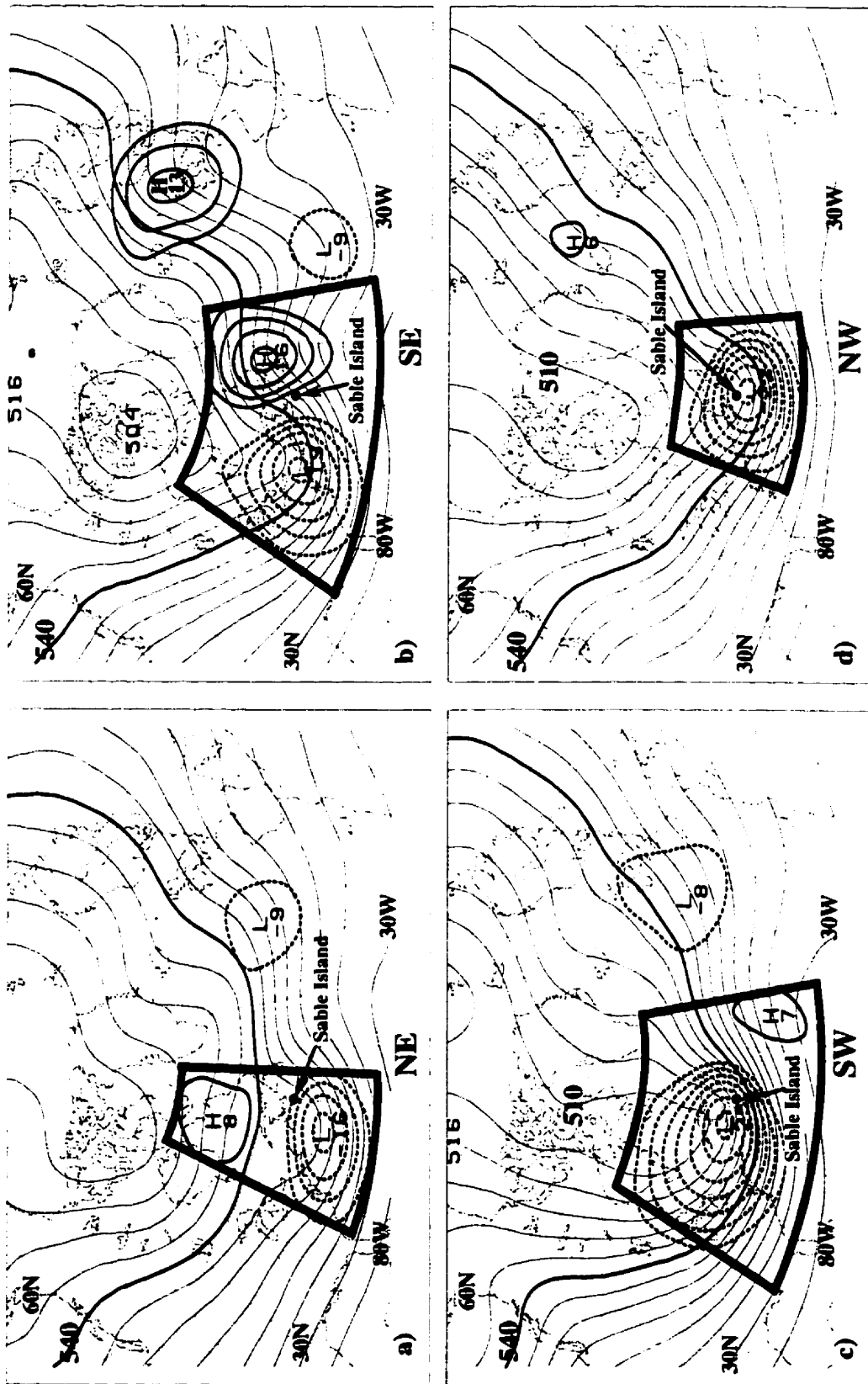


Fig. 4.1. Composite 500-hPa geopotential height (every 6 dam) and geopotential height anomalies [negative (dashed) and positive (solid) contoured every 3 dam]. The 0 and 3 (-3) dam positive (negative) anomaly contours are omitted for clarity. Panels a), b), c), and d) represent composites of the top 30 cases in the NE, SE, SW, and NW wind quadrants, respectively, at Sable Island. Areas outlined in bold represent regions in which the linear correlation analysis was performed.



Table 4.1 Number of cases in groups A, B, C, and D for each quadrant. The last column gives the number of cases in each quadrant not assigned to a group.

	A	B	C	D	outliers
NE	23	3	3	-	1
SE	22	4	2	-	2
SW	11	9	3	2	5
NW	24	3	2	-	1

Figure 4.1 reveals four distinctly different configurations in the 500-hPa height fields associated with each quadrant. These are summarised below.

- a) **NE** – There is very weak upper-level flow with the 540 dam contour only extending as far south as 50°N. The trough anomaly, weakest of all the quadrants, lies southeast of Nova Scotia in split 500-hPa flow.
- b) **SE** – There is a strong ridge downstream from the cyclogenetic trough southwest of Nova Scotia. A second prominent ridge lies over western Europe.
- c) **SW** – There is evidence of a large-scale cold surge as evidenced by the southward extent of the 516-hPa contour. The scale of the trough centred over Atlantic Canada is the largest of any quadrant.
- d) **NW** – An intense short-wave trough lies directly over Sable Island.

## 4.2 The NE quadrant

### a) *Characteristics of cyclones in NE group A*

Cyclones giving strong northeast winds to Sable Island tracked well offshore along the American eastern seaboard, passing south of Sable Island and east of Newfoundland (Fig. 4.2). At the time of the peak winds at Sable Island, centres lay on or near latitude 40°N and between 56°W and 64°W.

Cyclones giving high northeast winds to Sable Island had very modest deepening rates and in many cases were filling in the 12 hours preceding and following the peak winds (Table 4.2). Various authors have quantified an explosive deepening rate for mid-latitude cyclones (Hadlock and Kreitzberg 1988; Rogers and Bosart 1986; Sanders and

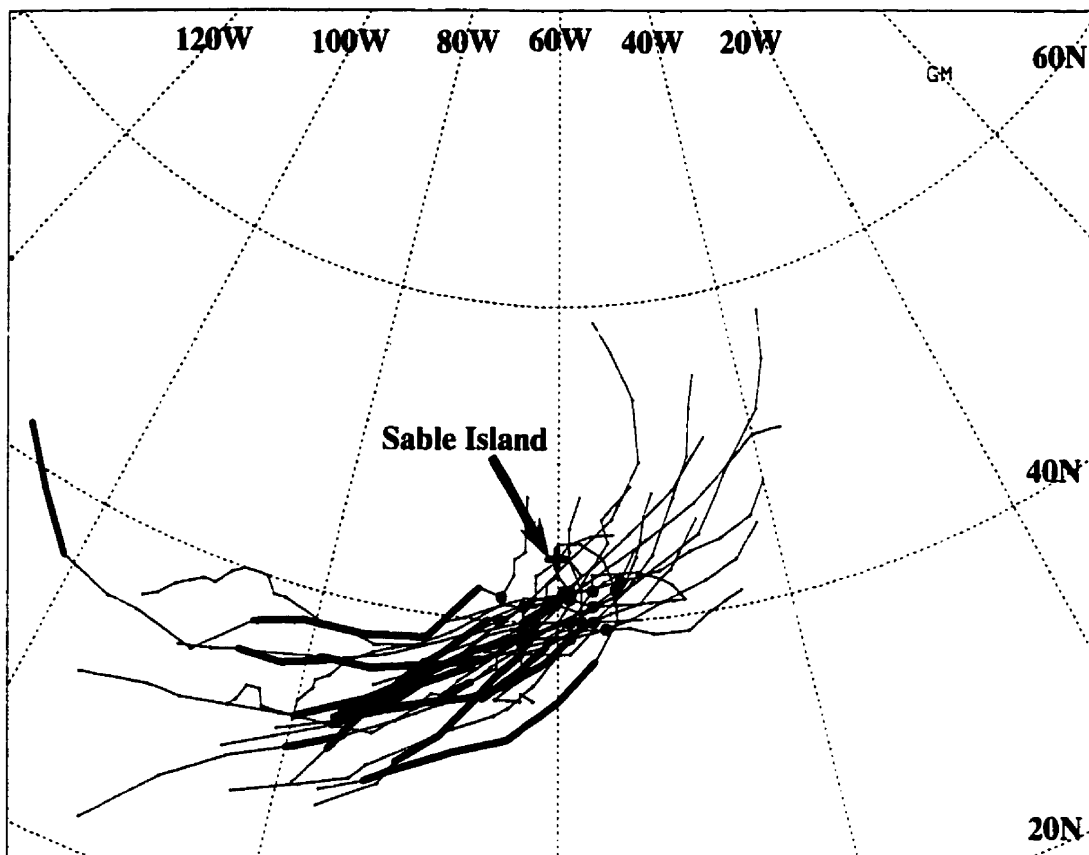


Fig 4.2. Tracks for 23 cyclones in NE group A. Lines in bold denote sustained 12 hour explosive deepening. Heavy dots mark cyclone center at H+00.

Gyakum 1980). Using the Sanders and Gyakum (1980) definition of a “bomb”, but for a 12 hour period, it was found that only one of the 23 NE group A cyclones was explosively deepening between H-12 – H+00. This is not surprising, given that 16 cases had a closed 500-hPa low by H+00 (not shown), and that phase speeds of these cyclones were generally low. It may be that the non-explosive nature of these systems is due to a seasonal effect, since 16 of the 23 cyclones occurred outside of the traditional winter period of December, January, February. One of these, the “Halloween” storm of October 1991, formed out of the circulation associated with hurricane Gloria (Avila and Pasch 1992). The high winds, which occurred all along the coast from Atlantic Canada to Georgia, were the result of an intense pressure gradient between this cyclonic circulation and a very strong high pressure system situated over Labrador. It will be seen later that the strong high pressure system over the Labrador area was a feature common to many of these high wind events.

*b) Composite evolution of NE group A*

Figure 4.3 gives a six day flow evolution of the 500-hPa geopotential height, 1000-500 hPa thickness, sea-level pressure fields, and associated anomalies associated with NE group A. At H-96 there is a significant 500-hPa trough over the eastern coast of the United States related to a surface composite cyclone near Cape Hatteras. Its existence is supported by a cold thickness anomaly to the southwest of the upper-level trough anomaly in northwesterly flow behind the surface cyclone. This feature and its attendant trough move northeastward along the coast, passing east of Sable Island and Newfoundland, and crossing the Atlantic. The associated upper trough anomaly reaches its maximum value at H-48 and has faded completely by H+00 near the west coast of Europe.

Several days prior to the HWE a significant ridge anomaly extends from the Davis Strait to Iceland. This feature is evident at H-160 (not shown) and can clearly be seen at H-96. There are actually two significant ridges, one over the Davis Strait and another near Iceland. The latter ridge is associated with weakening of the climatological Icelandic Low and persists until H+00 when it loses its significance. By H-48 the other

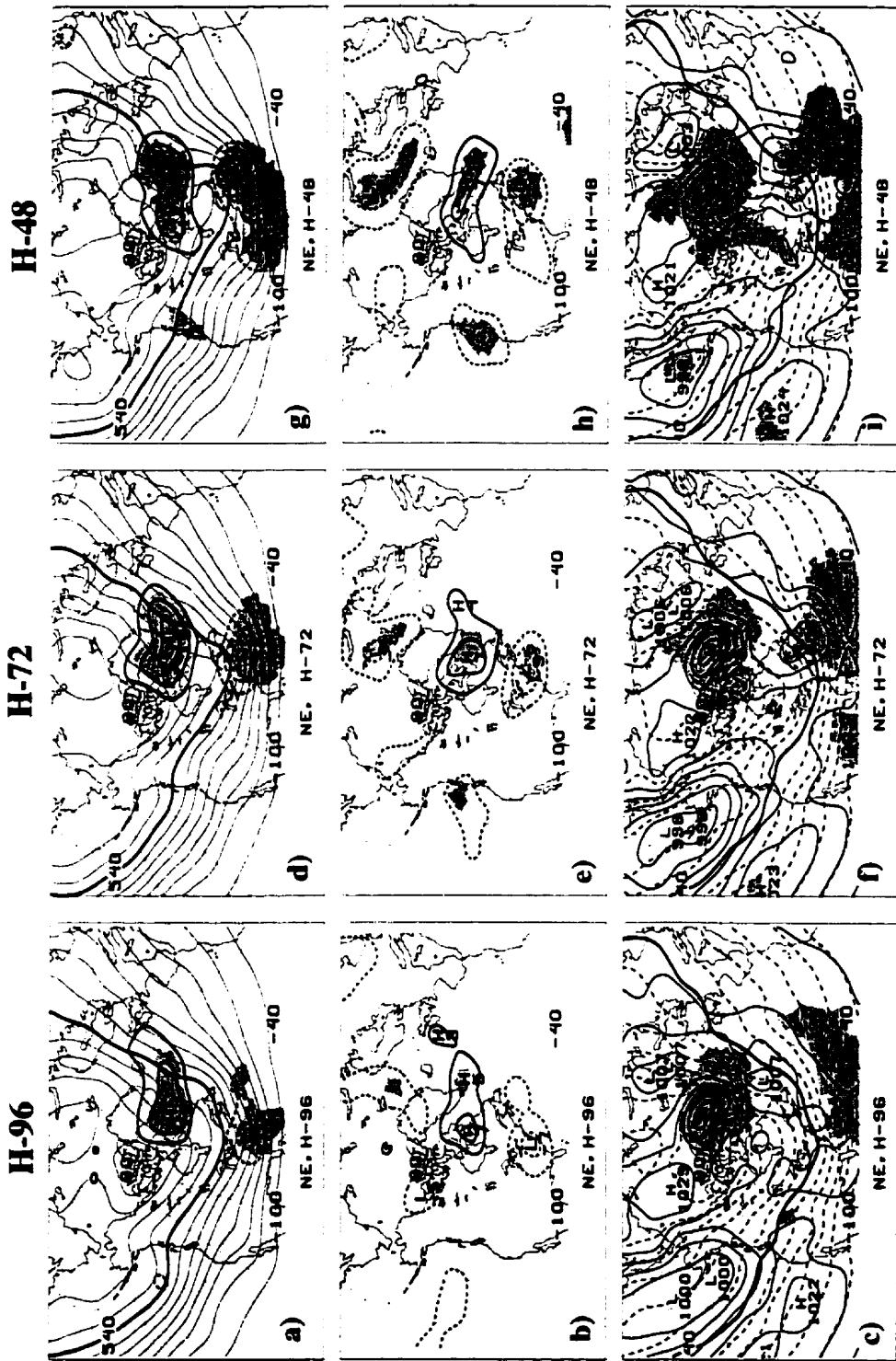
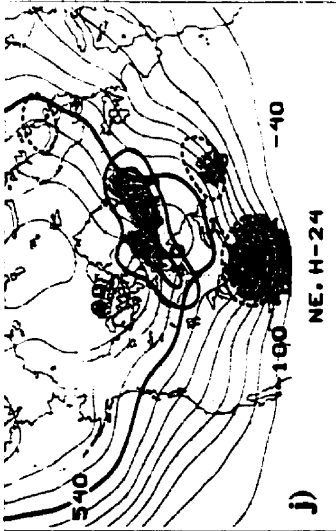
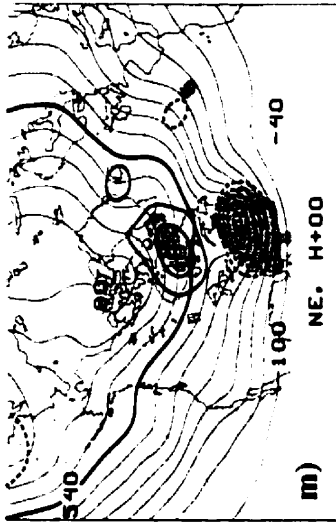


Fig. 4.3 Composite 500-hPa geopotential height (every 6 dam), height anomalies [every 3 dam, positive (negative) values solid (dashed), 0 and 3 (-3) contours omitted for clarity] in top three panels. Composite 1000-500 hPa thickness anomalies [every 3 dam, positive (negative) anomalies solid (dashed) with zero contour omitted for clarity] in middle three panels. Composite sea-level pressure (solid, every 4 hPa) and composite 1000-500 hPa thickness (dashed, every 6 dam with 540 dam contour in heavy solid) in lower three panels. Shading in all panels refers to statistical significance of anomalies at 95% confidence or greater as determined from two-sided Student's t-test. Panels a)-c), d)-f), g)-i), m)-o), and p)-r) represent composites at H-96, H-72, H-48, H-24, H+00, and H+24, respectively. Composites represent 23 cases in NE group A.

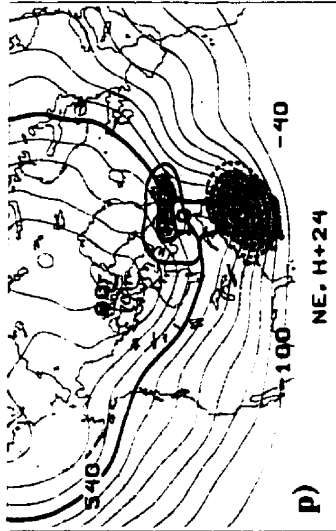
H-24



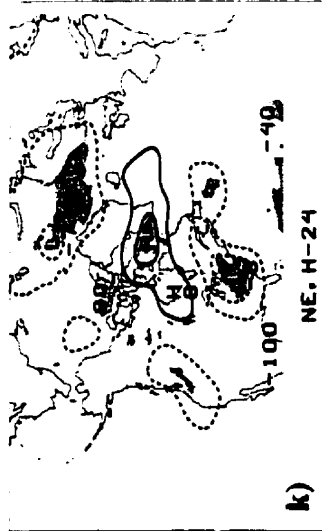
H+00



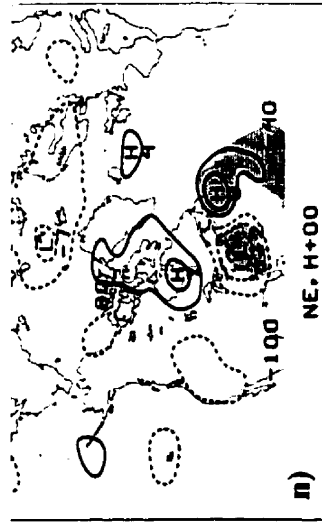
H+24



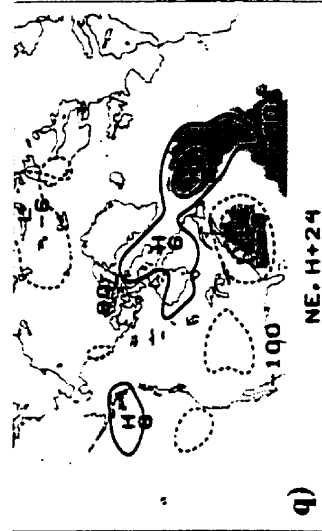
NE, H-24



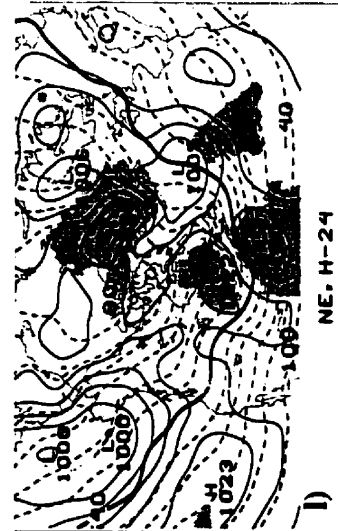
NE, H+00



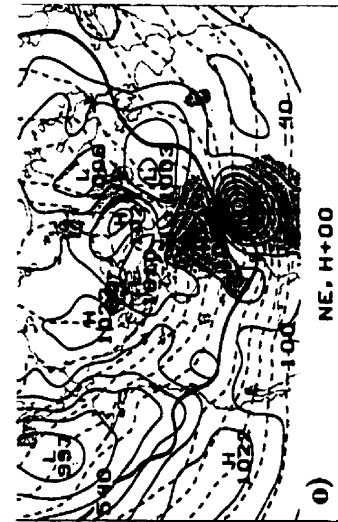
NE, H+24



NE, H-24



NE, H+00



NE, H+24

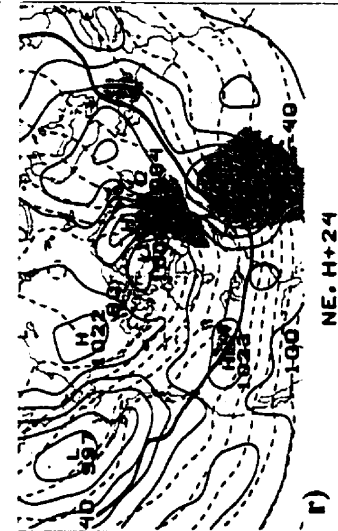


Fig. 4.3 (continued)

**Table 4.2 List of dates and peak wind speeds of each high wind event in NE group A. Also given are the deepening rates in the 12 hours preceding and following H+00. These are adjusted for latitude. The last column gives the average phase velocity of each cyclone in the 12 hours preceding H+00.**

NE-Group A							
Date in UTC				peak wind speed ( $\text{m s}^{-1}$ )	deepening rate (H-12 – H+00) (hPa/12h)	deepening rate (H+00 – H+12) (hPa/12h)	phase speed (H-12 – H+00) ( $\text{m s}^{-1}$ )
year	day	month	hour				
1980	06	January	06	20.6	-2.7	1.3	17.9
1980	08	February	12	19.4	-9.6	-6.8	12.4
1981	07	March	12	19.4	-1.4	0.0	4.0
1981	21	March	06	21.1	-1.3	9.1	11.0
1981	26	November	12	23.1	-1.3	4.0	9.5
1982	07	April	06	22.5	-1.3	1.3	14.1
1983	26	March	00	20.6	7.0	8.1	16.1
1983	25	October	12	23.6	-17.2	-6.5	21.3
1984	30	March	06	20.6	0.0	2.6	13.1
1986	12	May	06	19.4	-4.1	1.4	5.1
1986	20	August	12	20.6	-2.6	-1.3	7.7
1987	01	January	00	22.2	0.0	0.0	13.6
1987	27	January	00	21.1	1.3	2.6	20.9
1988	03	May	12	20.6	-9.4	-9.1	13.1
1988	15	December	00	20.0	2.7	6.5	13.1
1989	24	November	00	21.7	-10.6	-3.7	19.0
1991	11	March	18	19.4	-2.6	0.0	11.0
1991	16	March	00	19.4	-6.7	-8.1	7.9
1991*	29	October	06	25.8	--	-6.8	3.9
1992	01	February	18	21.2	1.3	6.3	7.8
1993	28	February	18	19.2	-2.7	2.7	6.5
1994	12	March	06	20.6	-3.9	0.0	10.0
1995	31	August	00	19.2	-10.6	-11.8	12.8

\*High winds resulted from cyclone which formed out of the remains of hurricane Gloria near H-06.

ridge anomaly becomes evident over Hudson's Bay associated with a surface anticyclone in northern Ontario. This feature drifts eastward to lie over northeastern Quebec at the time of the HWE and acts to retard the northward progression of the primary cyclone associated with the HWE, keeping it well offshore. Also related to the offshore track is the split in upper-level flow steering surface features in an easterly direction.

By H-72 the beginning of the cyclone responsible for the high winds at Sable Island is first seen as a weak trough over the Gulf of Mexico. This may be related to an active southern branch of the westerlies, as short-waves travel into southern California from the Pacific. There is evidence for this in Fig. 4.3f and Fig. 4.3i, although the upper-level short-wave is not easily detectable. By H-48 the primary cyclone forms near Cape Hatteras and moves slowly up the coast to lie just east of Sable Island by H+00 with a central SLP of 990 hPa. However, the thermal wave only amplifies modestly, and the strength of the thickness anomalies relative to the other wind quadrants is quite small, suggesting that overall baroclinicity is quite weak. This is not surprising, given the finding that only one of the cyclones in NE group A was explosively deepening at H+00. At H+00 there is also a clear split in the 500-hPa geopotential height field as the cyclone lies just downstream of a strong upper-level confluent zone. Six hours later the upper-level trough has closed off (not shown) while the central SLP of the composite cyclone reaches its lowest value of 989 hPa. This is in agreement with our finding that many of the cyclones composing the composite had reached maturity at this time and were moving slowly. Thereafter, the cyclone fills, moves slowly to the east of Newfoundland, stalls, and has lost its identity by H+48 (not shown).

Noting that both composite cyclones did not move north of Newfoundland, and that their associated upper-level troughs tended to track zonally across the Atlantic, there is the suggestion that NE HWEs sometimes occur during the negative phase of the North Atlantic Oscillation (NAO). This may be related to the split in upper level flow, explaining the positive 500-hPa height anomaly over the Iceland-Greenland region and the unusually weak northern component of the cyclone trajectory. The NAO generally has two modes, one in which the circulation over the Atlantic Ocean is either anomalously strong (positive phase), or anomalously weak (negative phase) (Rogers 1990). Rogers (1990) found that in the NAO's negative phase North Atlantic cyclones

have a more zonal track, in which storms generally follow the Gulf Stream along 45°N. He also found that in this mode there is anomalously high pressure between Greenland and Iceland. Dole (1986) described a pattern of strong anomalies of alternating sign in the 500-hPa height fields over the central North Atlantic as the Atlantic (ATL) pattern. When this pattern was in its negative phase with a strong negative anomaly around 45°N, there was a pronounced zonal orientation in the Atlantic storm path, which extended across the Atlantic near 40°N.

The significant features found several days in advance of NE HWEs suggest that these may have an element of predictability. The most dominant signal is ridging in the Davis Strait, and the presence of a precedent cyclone along the Atlantic seaboard. This predecessor cyclone was also found in the study by Lackmann et al. (1996) on signatures relating to explosive east coast cyclogenesis. However, it is unlikely that the cyclone responsible for the HWE is the result of secondary cyclogenesis along a trailing cold front (Snyder 1996; Browning and Roberts 1994), since there is little evidence of frontal troughing in our composites. There is evidence in Fig. 4.3f that suggests some of these systems are travelling in from the Pacific in the southern branch of the westerlies.

### **4.3 The SE quadrant**

#### *a) Characteristics of cyclones in SE group A*

Twenty cyclone centres were tracked in SE group A, since two of the 22 cases could not be explicitly linked to a cyclone. These two cases both shared the feature common to SE group A of a strong anticyclone southeast of Newfoundland. High winds in these two cases were identified to be the result of an intense pressure gradient between a surface trough south of Nova Scotia and the downstream anticyclone (not shown).

Cyclones giving strong southeasterly wind to Sable Island generally followed the Atlantic seaboard, tracking northeast to lie west of Sable Island at the time of the HWE. Only five of these cyclones had origins over land, in contrast to the composite cyclone track which originated west of the Great Lakes (Fig. 4.5). This contrast was even more



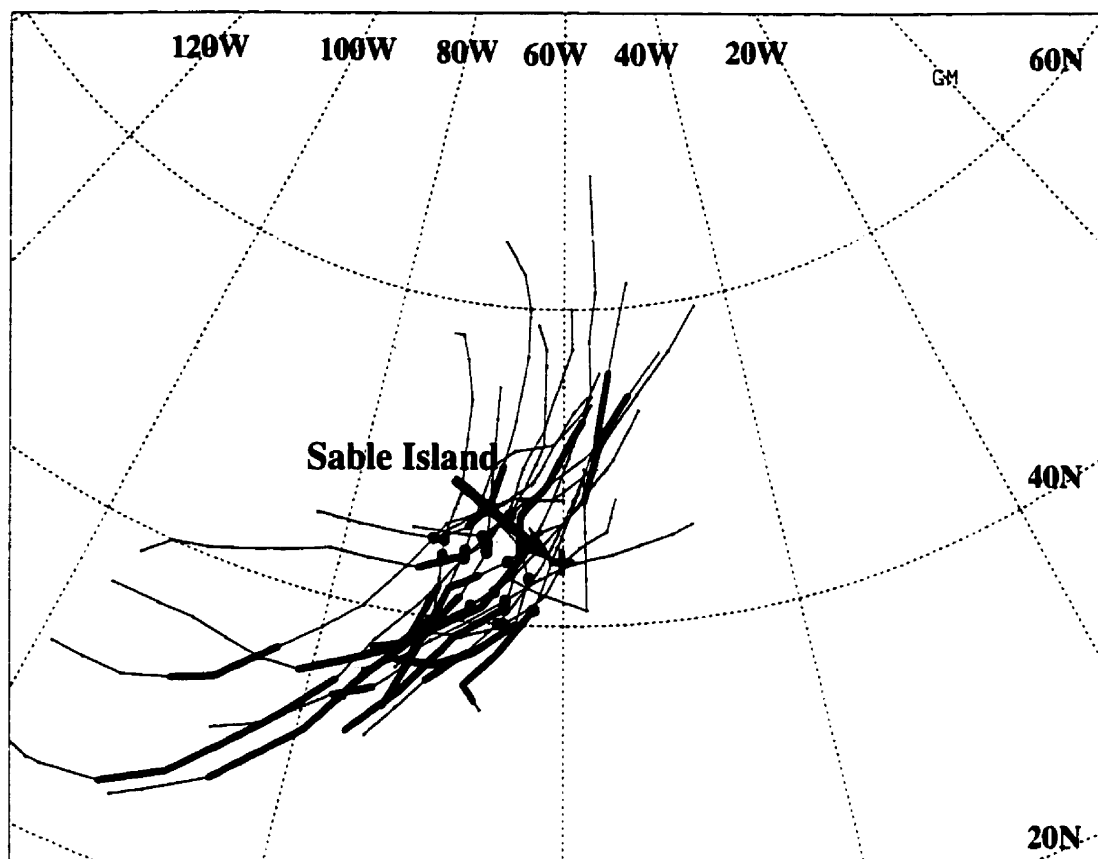


Fig. 4.4 As in fig. 4.2 but for 20 cyclones in SE group A.

pronounced when the composite cyclone track was examined at a temporal resolution of 12 hours (not shown). The discrepancy demonstrates the importance of verifying a composite cyclone track against the observed tracks. When we examined the composite cyclone track with a six hour temporal resolution it was evident that composite coastal redevelopment took place (to be discussed later in this section). This phenomenon was seen in many cases while tracking cyclones. In other instances there was simply a Great Lakes cyclone which tended to persist while a new centre spun up off the east coast.

At H+00 cyclones giving strong southeast winds to Sable Island lay in one of two distinct groups. One group had centres that lay south and west of the island in the ocean between 40°N and 44°N and 62°W and 70°W. These had a marine path as they tracked northeastward, crossing Nova Scotia and Newfoundland into the Labrador Sea. The second group lay north and west of the island between 45°N and 47°N. These cyclones (7, one of which was the March 1993 “superstorm”) generally followed the coastline as they took a more northward track, crossing Maine and New Brunswick into Labrador. What is characteristic of all 20 cyclones tracked in SE group A is the distinct northerly track they follow beyond the time of the HWE.

These cyclones were typically deepening, but not explosively, in the twelve hours preceding H+00. Despite this, their phase speeds during this time were quite modest, with an average speed of  $13.6 \text{ m s}^{-1}$  (only four had phase speeds of less than  $10 \text{ m s}^{-1}$  during this time). As we will see later in this section, the fairly rapid movement was likely due in part to the strong baroclinicity that characterised these systems.

#### *b) Composite evolution of SE group A*

Three key surface features are identified at H-96 in SE group A (Fig. 4.5). The first feature is a composite cyclone near Sable Island associated with a weak 500-hPa trough anomaly (T1) and cold air over southeastern Canada. T1 follows a nearly zonal trajectory along 40°N and remains statistically significant for the entire six day composite evolution, losing its identity by H+96 (not shown) near the Greenwich meridian. Its barotropic structure can be seen with the near collocation of the associated cold anomaly. The composite cyclone tracks east of Newfoundland and amalgamates with the pre-

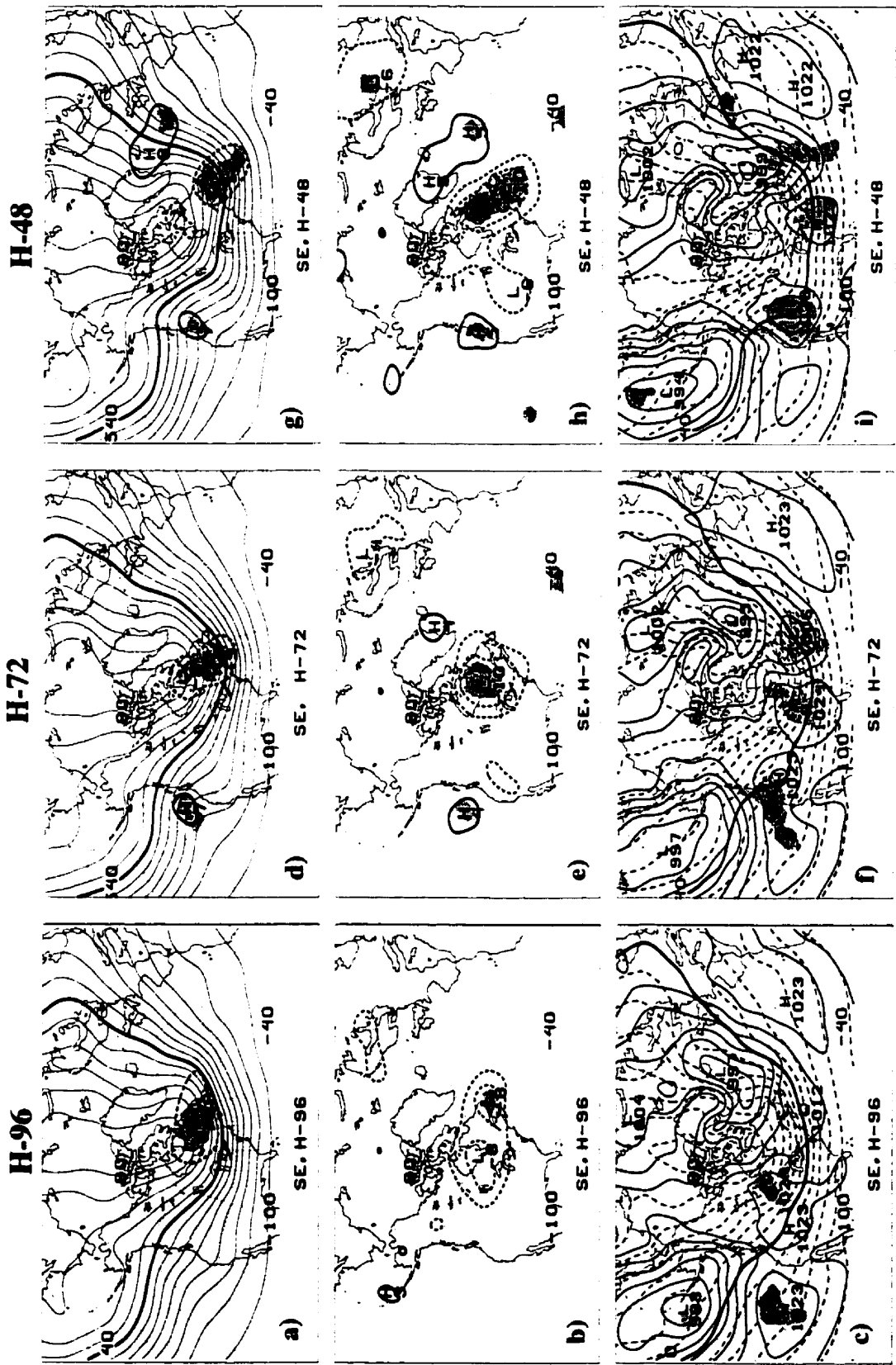


Fig. 4.5 As in fig. 4.3 but for composite of 22 cases in SE group A.

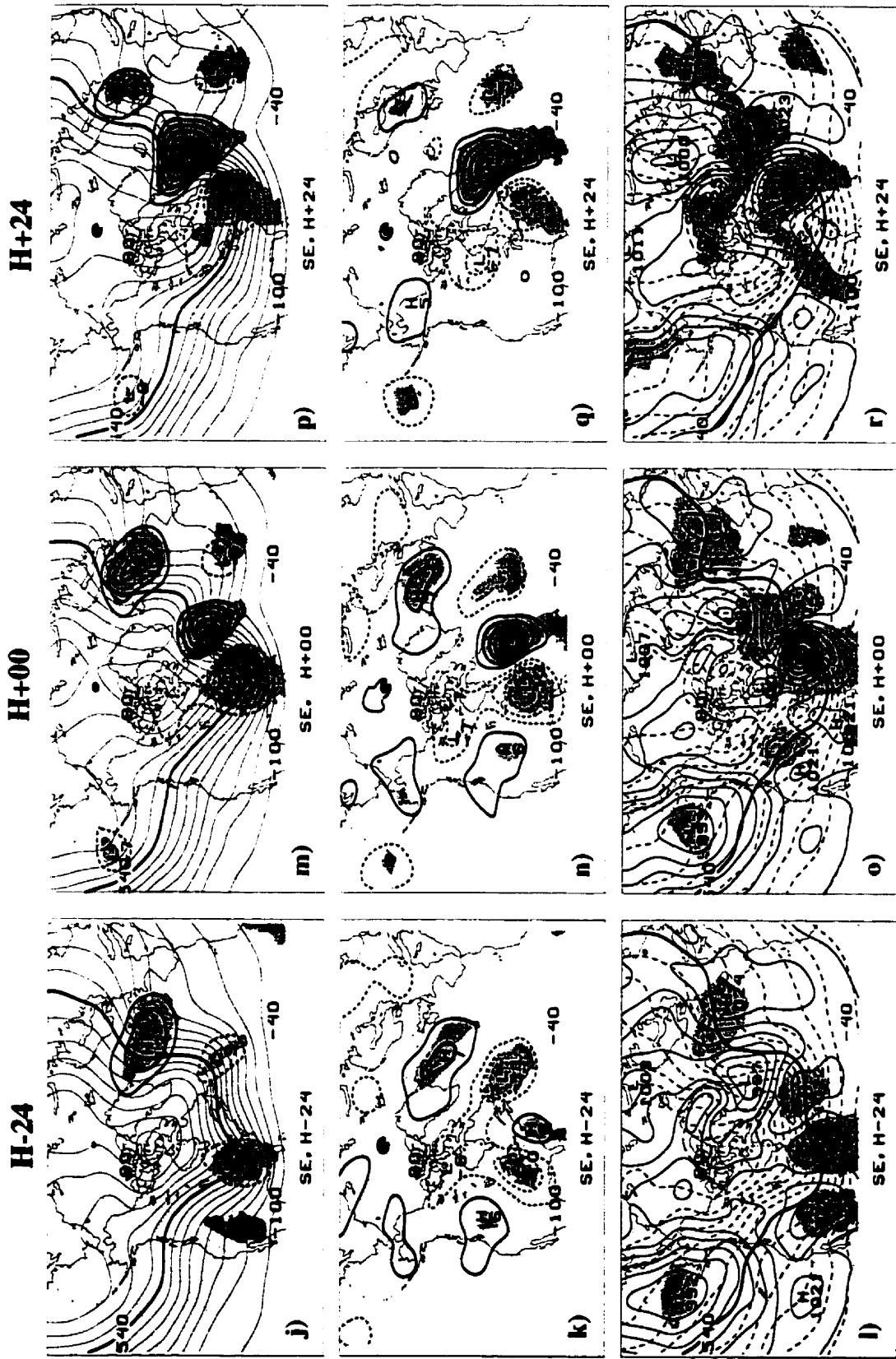


Fig. 4.5 (continued)

**Table 4.3 As in Table 4.2 but for SE group A.**

				<b>SE-Group A</b>			
Date in UTC				peak speed of	deepening rate	deepening rate	phase speed
year	day	month	hour	wind ( $\text{m s}^{-1}$ )	(H-12 – H+00) (hPa/12h)	(H+00 – H+12) (hPa/12h)	(H-12 – H+00) ( $\text{m s}^{-1}$ )
1979	22	January	06	21.7	3.7	4.8	16.0
1979	17	December	18	25.8	-18.4	-4.7	21.7
1980	05	April	12	19.4	-1.2	3.5	12.2
1980	17	December	18	19.4	-4.0	-3.8	14.4
1981	08	January	06	19.2	-17.6	-11.3	8.9
1981	17	March	18	20.6	2.5	11.0	15.1
1981	07	November	12	19.4	-2.4	4.7	5.4
1982	24	January	18	21.1	-10.7	-1.1	15.7
1983	08	February	12	20.6	-1.3	0.0	9.3
1984*	22	December	18	22.5	--	--	--
1987	23	January	12	20.0	-1.2	3.5	18.4
1987	01	February	00	22.5	-6.7	-6.6	6.5
1988	13	February	12	22.5	-8.6	-3.5	11.0
1988	02	November	18	20.6	0.0	2.4	10.3
1988	18	December	06	20.0	-10.6	-4.9	16.3
1989	25	March	18	19.4	-9.1	-11.4	14.1
1989*	08	August	06	27.2	--	--	--
1990	17	December	00	19.4	-5.0	0.0	10.7
1993	14	March	12	20.0	1.2	9.5	19.3
1993	28	October	00	19.4	-10.8	-9.0	14.4
1994	11	December	18	19.2	-9.8	-11.7	18.2
1995	05	February	12	24.2	-4.9	4.7	15.0

\*High winds at H+00 were not due to a cyclone.

existing area of low pressure in the Labrador Sea at H-48. Also of interest is the ridge anomaly downstream from T1 that develops at H-48 and drifts eastward to lie over western Europe at H+24. This is vertically collocated with a surface anticyclone.

Farther west the second key feature at H-96 is evident—a composite anticyclone (A1) over Saskatchewan/Manitoba which will play a strong role in producing the high winds over Sable Island. The third key feature at this time is a composite anticyclone in the eastern Pacific off the coast of California (A2). It appears to redevelop east of the California coast and tracks south toward Mexico. As it does so there is evidence of amplification in the upper-level height and thickness field by H-48 as a trough emerges out of northwesterly flow, a situation found by Sanders (1988) to be favourable for upper-level trough genesis. A1 has travelled south of the Great Lakes to lie just off the coast of North Carolina. Its shallow nature is evidenced by the lack of any associated statistical anomalies in the 500-hPa geopotential height field. Between A1 and A2 a clearly defined deformation zone has now formed over the central United States.

Twenty four hours later, at H-24, a strong upper-level trough anomaly extends from James Bay to Florida as a broad area of low pressure develops, stretching from south of the Great Lakes to the Florida peninsula. This is linked to a composite cyclone that forms in the deformation zone between A1 and A2. A thermal wave develops as southeasterly flow is enhanced between the cyclone-anticyclone couplet along the Atlantic coast. The environment is now favourable for coastal frontogenesis, as there is some evidence of ridging over the Appalachians. Coastal frontogenesis is a phenomenon which often occurs along the New England coast in early and middle winter when ocean temperatures are relatively warm compared to the land and a cold anticyclone approaches from the north. As the cold air flows south or southwestward it becomes trapped by the Appalachian Mountains, unable to climb over them. At the same time a trough approaches from the west and the result is to increase the onshore easterly flow. Temperature gradients tighten at the coast and coastal frontogenesis commences (Bluestein 1993).

Six hours later at H-18 a new composite cyclone (CP) forms off the Carolina coast (not shown), indicating that several cases composing the composite experienced coastal re-development, a phenomenon noted during the tracking of several of these

cyclones. By H+00 an intense pressure gradient exists over Sable Island between CP and the downstream anticyclone. The strong baroclinicity associated with this coupled cyclone-anticyclone pair is manifest in the thickness anomaly and 500-hPa anomaly fields at this time. In just 24 hours a 17 dam 500-hPa ridge anomaly develops, while a 13 dam (16 dam) negative (positive) thickness anomaly also develops. This translates into approximately a 15°C horizontal temperature gradient anomaly.

By H+24 the upper-level trough weakens considerably as it acquires a negative tilt and CP fills to 992 hPa. The weakening may be related to decreased cyclonic vorticity advection, as the downstream ridge strengthens to a 21 dam anomaly and slows the advent of the cyclogenetic trough. Deep tropospheric warming (as manifest in the thickness fields) is helping to build this ridge in the presence of strong warm air advection. It is also very likely that latent heat release in moist southerly flow is playing an additional role in strengthening the downstream ridge. The ridge anomaly remains strong 24 hours later while drifting eastward to cover much of the central North Atlantic Ocean. The climatological Icelandic Low is replaced by a composite ridge, while the cyclogenetic trough vanishes. The only remaining feature of CP is a weak surface trough in the Davis Strait. In the following 48 hours the central Atlantic ridge weakens to a 10 dam anomaly east of Greenland along 50°N, while remaining statistically significant.

Bell and Bosart (1989), hereafter referred to as BB89, studied the large-scale atmospheric structure accompanying New England coastal frontogenesis for the period 1964-1972. Their composite study of 11 coastal frontogenesis events yielded very similar results to our findings in the SE wind quadrant. They documented the existence of an anticyclone 48 hours before the onset of coastal frontogenesis that travelled eastward across the Great Lakes toward northern New England and Nova Scotia, similar to our A1. BB89 also found a high pressure centre which developed over the central United States and moved southeastward to the Gulf coast, similar to our A2. A composite cyclone formed over the southeastern United States 12 hours prior to the onset of coastal frontogenesis and moved to southeastern New England in the next 24 hours. This agrees very well with the cyclone which we first noticed in the vicinity of the Great Lakes at H-36 (not shown) and which reformed off the coast 24 hours later as strong

geostrophic southeasterly flow developed ahead of the system in concert with the downstream anticyclone.

The behaviour of our trough-ridge couplet southwest of Greenland also resembles that of BB89, though their cyclogenetic trough developed a closed circulation 24 hours following the onset of coastal frontogenesis. BB89 also suggest the existence of a double trough-ridge couplet (their Fig. 3c) over the central Atlantic Ocean at the time of major coastal development. However, they do not show a significant coastal cyclone preceding coastal frontogenesis similar to our finding at H-96. This may be because their period of study extended to 48 hours prior to the onset of coastal frontogenesis, while our study extends to 96 hours prior to a HWE. The strong Atlantic ridge found in this study southwest of Greenland is a feature also found in the Lackmann et al. (1996) study of explosive cyclogenesis over the western North Atlantic ocean.

Because our study documents composite features over a six day span, the continuity and significance of features is captured with more clarity than either BB89 or L96. However, these studies complement ours and strengthen the assertion that an anticyclone moving ahead of major east coast cyclones is an integral player in conditioning the coastal environment of the southeastern United States for strong coastal lows. Once these cyclones develop, the downstream ridge amplifies even further in strong southerly flow and latent heat release. This serves to retard the eastward progression of the cyclone, which subsequently dissipates. The large-scale ridge anomaly over the central Atlantic may act as a block as it retains its strength several days after the cyclogenetic trough has disappeared.

#### **4.4 The SW quadrant**

Two main groups were identified in the SW quadrant, with 11 cases in group A and 9 cases in group B. The associated cyclone tracks are given in Fig. 4.6. Because two main groups were identified with the remaining ten cases not falling into a major group, it is clear that HWEs in this quadrant are difficult to classify, possessing large variance in both structure and origin. Many of these systems followed a continental track, while several others were marine systems (Fig. 4.6).



### *a) Characteristics of cyclones in SW group A*

Cyclone tracks associated with SW group A possessed very little scatter up to H+00, with the single exception of a continental cyclone originating in the lee of the Canadian Rockies (Fig. 4.6a). They primarily followed a marine track originating in Texas or the Gulf of Mexico and travelled northeastward along the American coast to lie just west of Sable Island over Nova Scotia or the Gulf of St. Lawrence at H+00. Their movement was generally rapid, with an average phase speed of  $15.2 \text{ m s}^{-1}$  in the twelve hours prior to H+00 (Table 4.4). Only one of the 11 cyclones--which happened to be the only cyclone filling--had a phase speed below  $10 \text{ m s}^{-1}$  during this time (Table 4.4). Because of the minimal scatter in these cyclone tracks, we can be fairly confident of composite results based on these 11 cases.

Unlike the majority of cyclones in NE and SE group A, all of these cyclones continued to develop beyond H+00, although two began to fill after H+06 (not shown). They were also quite intense, with five of the 11 cyclones deepening explosively in the twelve hours prior to H+00 (Table 4.4). In fact, eight had deepening rates exceeding 1.5 bergerons at some point in their life cycle (two exceeded 2.0 bergerons). By H+00, all 11 cyclones had a central SLP value below 990 hPa, with seven possessing a value below 980 hPa (not shown). This is consistent with the composite cyclone having a central SLP of 978 hPa at H+00 (Fig. 4.7o), although this low value is also due to the small scatter of cyclone centres at this time. The explosive nature of most of these cyclones prior to H+00, and their low central SLP values, partly explain why on average we found the highest wind speeds in the SW quadrant.

### *b) Composite evolution of SW group A*

Figure 4.7 gives the six day flow evolution of composite fields associated with the cyclones in SW group A. The dominant feature at H-96 is an enhanced Aleutian Low in the eastern Pacific, and a downstream positive ridge anomaly over western North America which remains quasi-stationary and retains its significance until H+24. Over

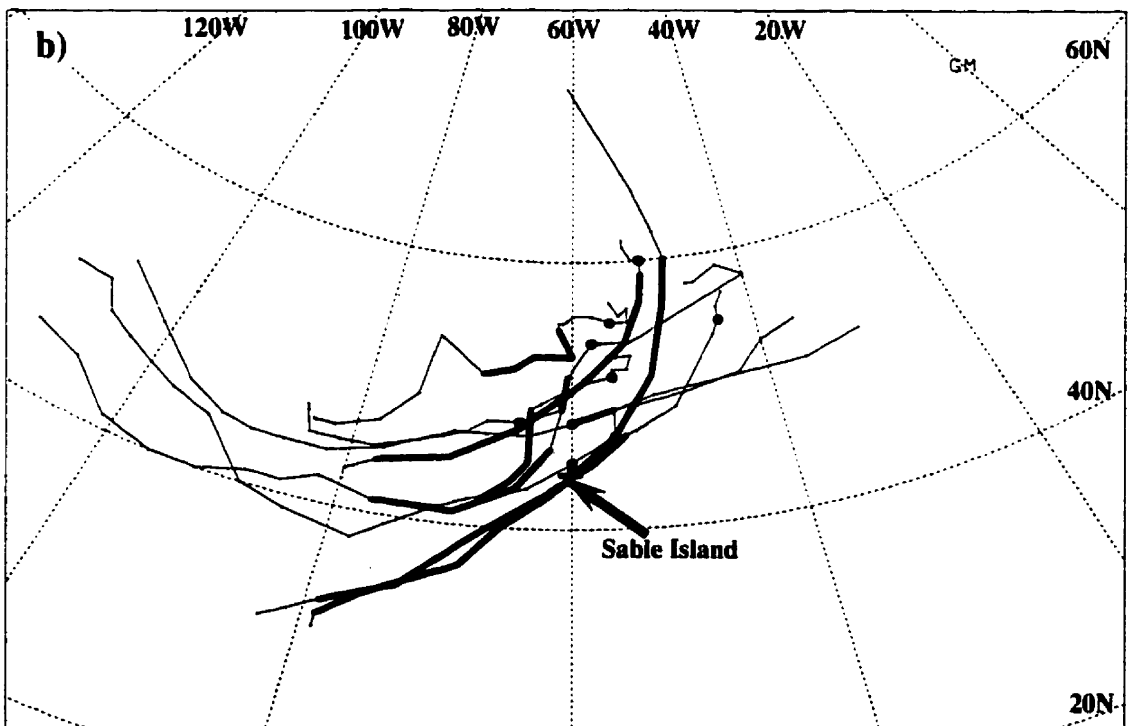
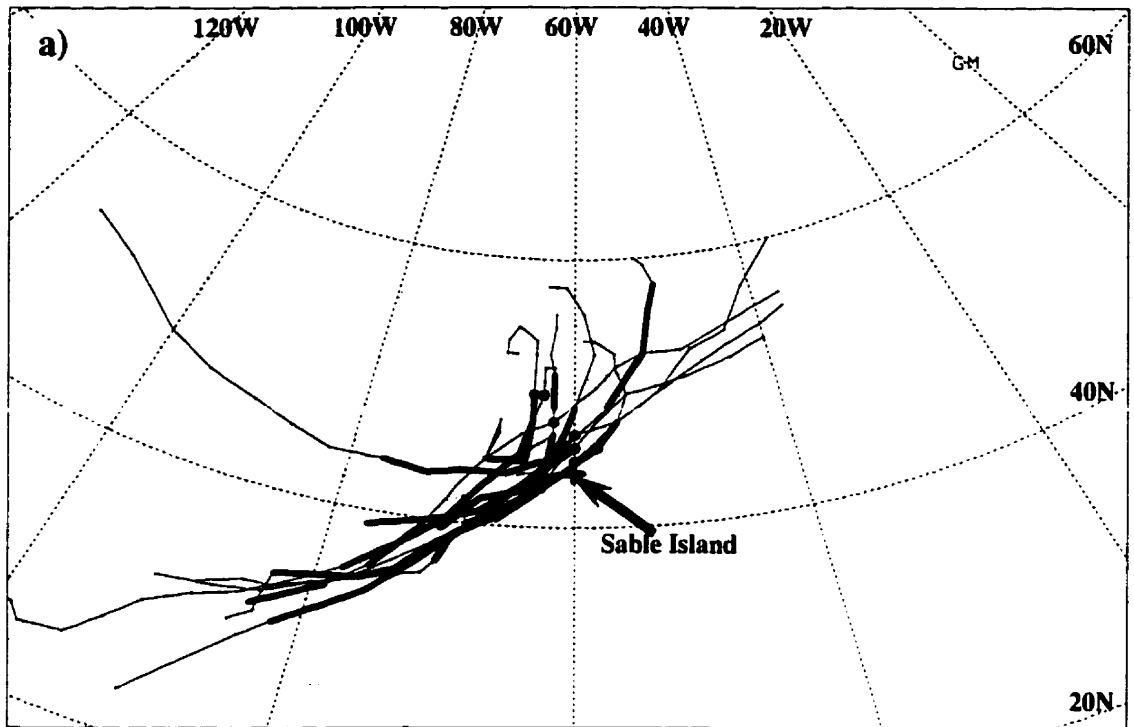


Fig. 4.6 As in fig. 4.2 but for a) 11 cyclones in SW group A and b) 9 cyclones in SW group B.

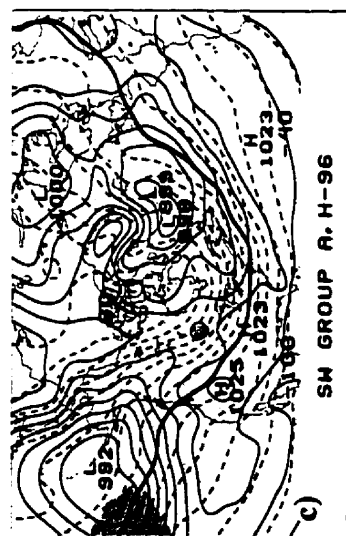
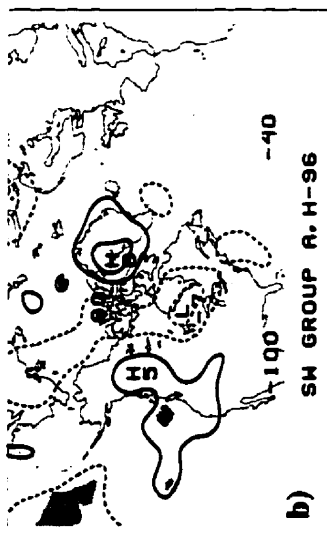
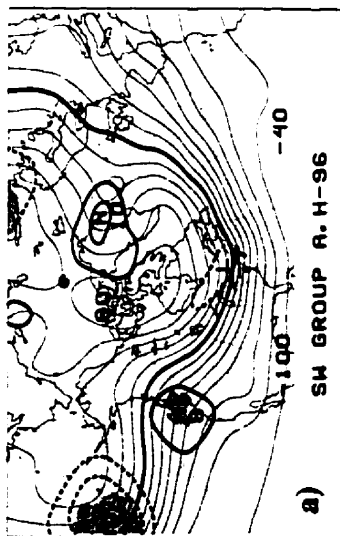
eastern North America there is a deep trough. This pattern resembles the positive phase of the Pacific-North American (PNA) pattern (Wallace and Gutzler 1981) and was also identified by L96 as a persistent feature in the period bracketing explosive cyclogenesis in the western North Atlantic ocean. Related to the positive 500-hPa ridge anomaly over western North America is a strengthening anticyclone east of the Rockies. By H-48 this feature has become significant and is drawing cold air from the Northwest Territories deep into the central continent. This can be linked to a digging trough at H-48 as the thermal wind develops a strong meridional component and strengthens over the Prairie provinces.

By H-24 the digging trough has reached the east coast while strengthening to a negative 19 dam anomaly. At the same time a closed polar vortex centred over Hudson Bay begins to sink southward. The result is an intense cold air outbreak over the eastern United States that acts to enhance the coastal baroclinic zone as cyclonic development commences. A warm anomaly in southerly flow from the coastal cyclone begins to form just east of Cape Hatteras. The situation is highly favourable for explosive cyclogenesis as the cyclone now lies over a low level baroclinic zone with a well defined confluent zone in the thickness pattern (Sutcliffe and Forsdyke 1950). It is also accessing the cold arctic air west of the coastal baroclinic zone. Twenty four hours later the composite cyclone has deepened a remarkable 24 hPa (a composite bomb) and attained a central SLP value of 979 hPa over Cape Breton, Nova Scotia, while giving very strong geostrophic wind to Sable Island.

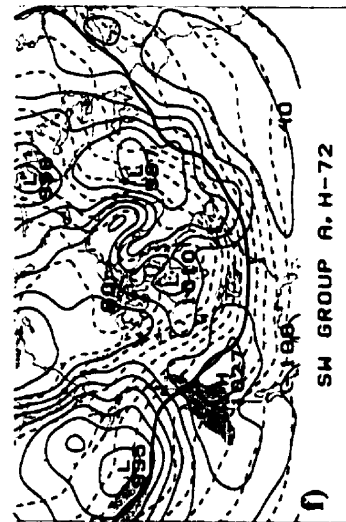
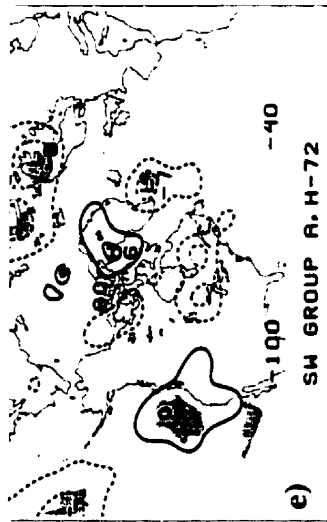
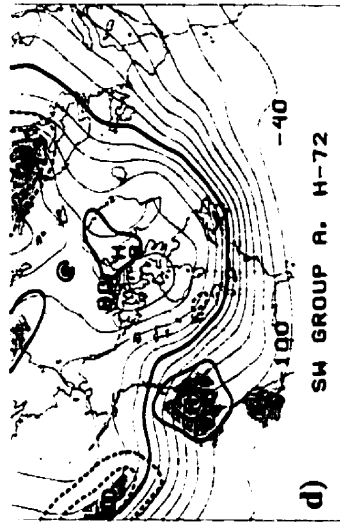
A planetary-scale trough covers much of eastern North America as the composite cyclone reaches maturity and becomes vertically co-located with the upper low at H+24. Cold air lingers over the east coast until H+96 (not shown) while the polar vortex drifts east to lie over the Labrador sea, setting up large-scale cyclonic circulation over much of eastern Canada and maintaining a low-frequency cold surge.

Another interesting feature is the persistent upper-level height anomaly over the extreme northern regions of Canada. Its barotropic nature can be seen by the warm anomaly in these regions and is most pronounced between H-24 and H+24. This is consistent with Sanders (1988) study of thickness fields related to east coast explosive cyclogenesis. He suggested that there is polar warming coincident with cold surges

H-96



H-72



H-48

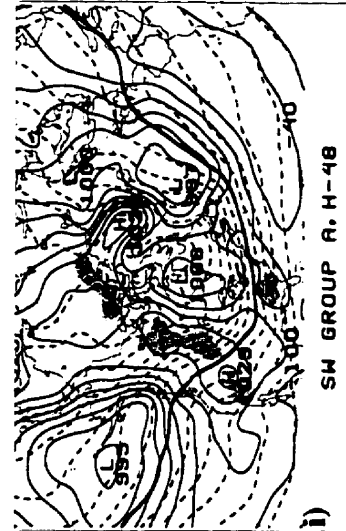
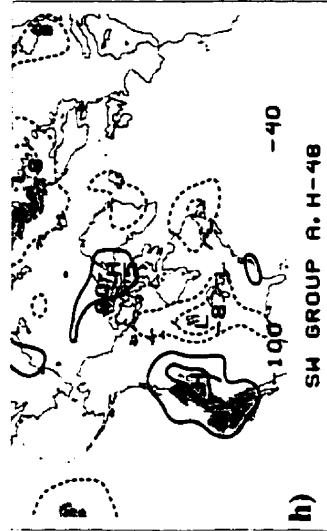
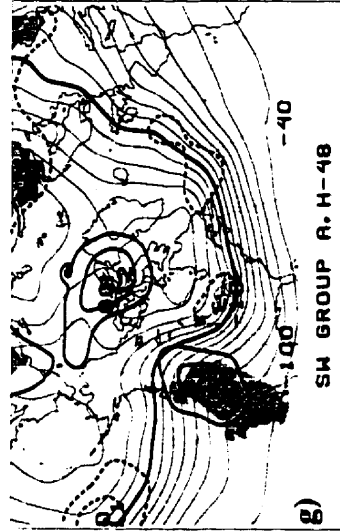
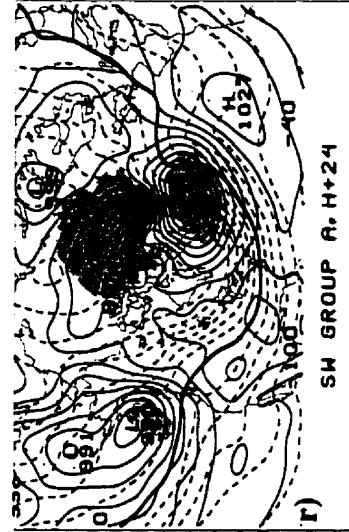
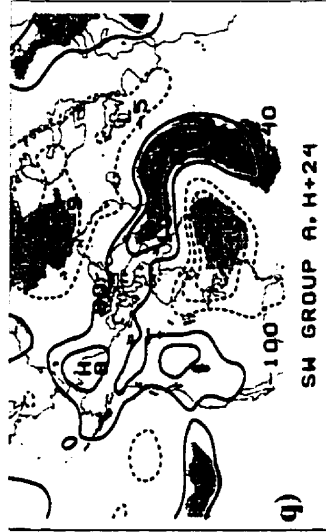
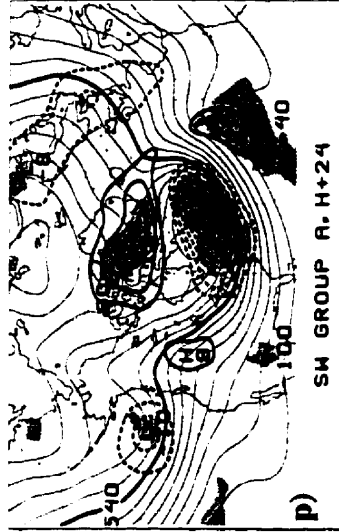
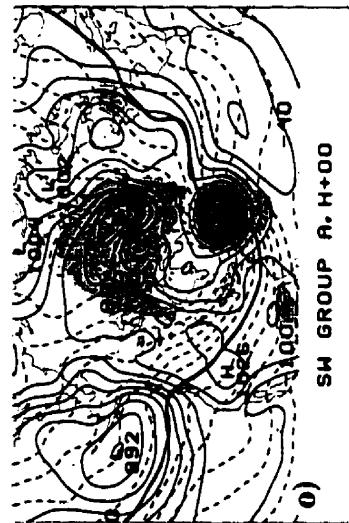
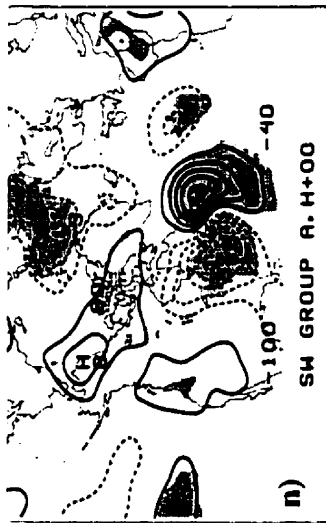
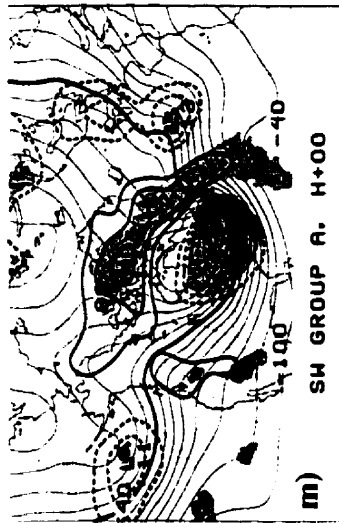


Fig. 4.7 As in fig. 4.3 but for composite of 11 cases in SW group A

H+24



H+00



H-24

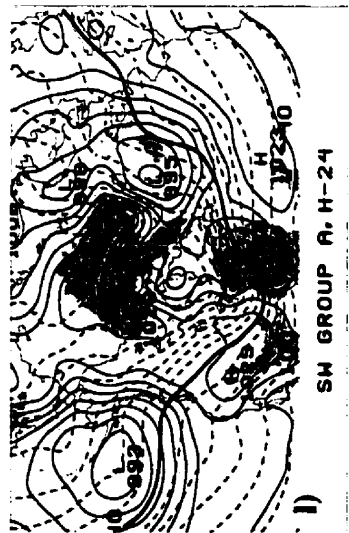
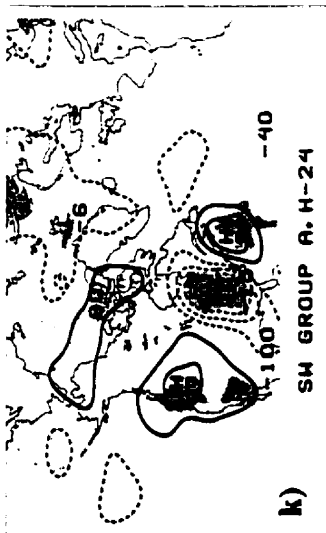
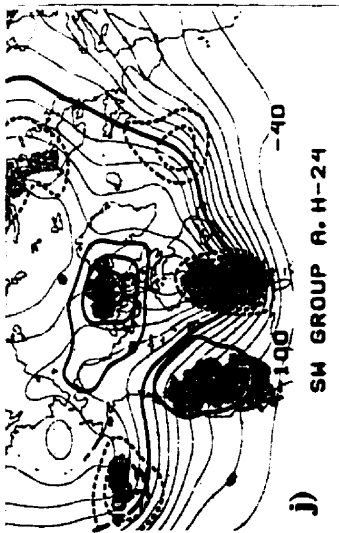


Fig. 4.7 (continued)

**Table 4.4 As in Table 4.2 but for SW group A.**

				<b>SW-Group A</b>			
Date in UTC				peak speed of	deepening rate	deepening rate	phase speed
				wind	(H-12 – H+00)	(H+00 – H+12)	(H-12 – H+00)
				( m s <sup>-1</sup> )	(hPa/12h)	(hPa/12h)	( m s <sup>-1</sup> )
year	day	month	hour				
1981	03	January	00	24.7	-16.5	-11.8	17.3
1981	17	December	06	26.7	0.0	-5.6	13.1
1982	15	January	18	28.3	-12.0	-4.7	21.6
1985	06	January	00	26.1	-6.1	-3.5	16.8
1985	21	January	18	20.6	-11.3	-10.8	18.5
1986	14	January	12	23.1	-17.1	12.6	18.3
1988	05	February	12	21.7	-13.2	-11.5	5.1
1988	21	April	06	23.6	3.6	13.0	13.3
1989	21	January	18	25.3	-7.1	-4.7	19.7
1990	12	November	00	20.1	-9.0	-4.5	12.9
1993	31	December	00	28.9	-13.2	-9.3	10.9

**Table 4.5 As in Table 4.2 but for SW group B.**

				<b>SW-Group B</b>			
Date in UTC				peak speed of	deepening rate	deepening rate	phase speed
				wind	(H-12 – H+00)	(H+00 – H+12)	(H-12 – H+00)
				( m s <sup>-1</sup> )	(hPa/12h)	(hPa/12h)	( m s <sup>-1</sup> )
year	day	month	hour				
1979	09	December	06	20.6	-7.0	-14.9	14.1
1980	25	January	12	23.1	-5.5	1.1	12.6
1982	19	January	06	22.5	9.5	1.1	5.8
1983	25	December	12	23.6	-16.6	-21.0	15.0
1984	26	December	18	23.6	2.0	6.0	7.7
1986	07	January	12	20.6	2.1	10.7	6.0
1988	21	March	12	22.2	-3.2	7.3	18.1
1993	12	March	00	21.7	-2.4	-7.1	18.5
1993	27	December	00	25.8	-2.3	0.00	9.1

related to the most extreme cyclogenesis events over the western Atlantic. Finally, another persistent feature throughout the composite evolution is anomalous cold over Siberia.

Konrad and Colucci (1989) found a pattern similar to our composite 500-hPa geopotential height field at H-96 several days prior to an intense cold air outbreak in January 1977 affecting much of the southeastern United States. This strongly resembled that of the PNA pattern. They also found that intense cyclogenesis occurred following periods of major cooling across southeast North America. The three most intense cold air outbreaks during their period of study were linked to strong bombs (Sanders 1986) having a deepening rate exceeding 2.0 bergerons along the east coast. These cyclones all occurred following the onset of a cold air outbreak.

Evidence from our composite for SW group A suggests that the arrival of very cold air over the warm waters off the east coast may be a factor in the extra intensity of these systems. Manobianco's (1989) composite study of explosive east coast cyclogenesis over the west-central Atlantic Ocean found that strong upper tropospheric forcing is enhanced by a highly destabilised lower troposphere. This supports studies on the Presidents' Day storm, during which there were strong latent and sensible heat fluxes from large air-sea temperature contrast (Chou and Atlas 1982; Uccellini et al. 1987).

Konrad and Colucci (1989) also found that when cyclones did follow the onset of a cold air outbreak, the spatial scales tended to be much larger. Our results for SW group A are in agreement with this finding. Major coastal cyclogenesis began to commence in our composite only after a strong cold anomaly of a negative 15 dam had reached the east coast. The scale of this negative thickness anomaly was nearly 30° in longitude and persisted for the next five days.

### *c) Characteristics of cyclones in SW group B*

There were nine cyclones in group B, seven of which followed a continental track and two a marine track. Figure 4.6b shows the high degree of scatter in these tracks and of the cyclone centres at H+00. Only one of the cyclones—a marine system—was deepening explosively in the twelve hours prior to H+00. The high variability of these

### SW Group B

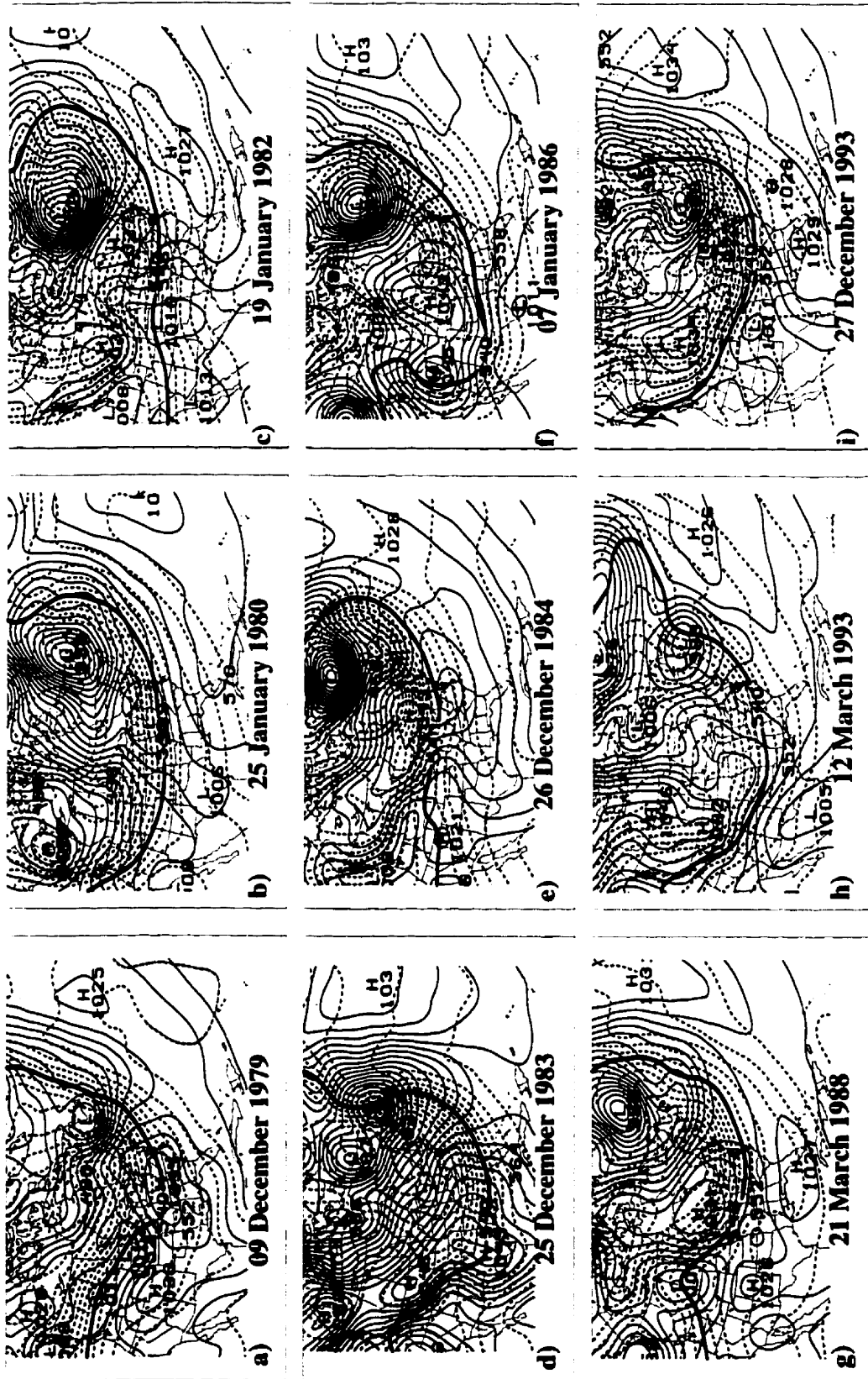


Fig. 4.8 Sea-level pressure (contoured every 4 hPa; solid lines) and 1000-500 hPa thickness (contoured every 6 dam; dashed lines) for each case in SW group B at H+00. The 540 dam thickness contour is denoted by the heavy solid line. Dates for each case are as indicated in panels a) to i).



systems would make a six day composite evolution a suspect method of study and hence it will not be shown.

Figure 4.8 shows the H+00 SLP and 1000-500 hPa thickness fields for the nine cases in SW group B. The most interesting feature common to all of these cases is the intensity of the thermal wind south of the Atlantic provinces. Clearly a cold surge is related to SW group B as well as SW group A. However, the synoptic pattern responsible for the cold surge in these cases is much more complex. For four of the cases a typical synoptic-scale cyclone north of Sable Island is responsible for the high winds. One of these, a marine cyclone giving high winds on 24 December, 1983, had remarkable sustained explosive deepening from 32°N to 60°N, with a maximum value of 2.8 bergerons. This was found by Konrad and Colucci (1989) to be related to the most intense cold air outbreak during their period of study. Of particular interest with this case is the anticyclone in the Yukon with a central SLP of 1053 hPa maintaining intense cold air advection over most of Canada and the United States. The remaining five cases are related to very deep cyclones with extremely large spatial scales far to the north of Sable Island, all of which tracked across the continent. In two of these cases the high winds appear to be related to a trough imbedded in the much larger-scale cyclonic circulation.

We can thus say that although there is a high degree of variability in the atmospheric states relating to SW HWEs, they generally are accompanied by intense cold surges. Moreover, the related cyclones tend to follow equally either a marine or continental track. What is also surprising is that the cyclonic circulation responsible for the high winds may in some cases have centres located far to the north of Sable Island.

#### **4.5 The NW quadrant**

##### *a) Characteristics of cyclones in NW group A*

Of the 24 cyclone tracks shown in Fig. 4.9, 10 originated over land. The remainder originated over the ocean and tracked northeastward well to the east of the coastline. At the time of the high winds at Sable Island, all cyclone centres lay east of Sable Island, generally along an axis oriented from southwest to northeast between

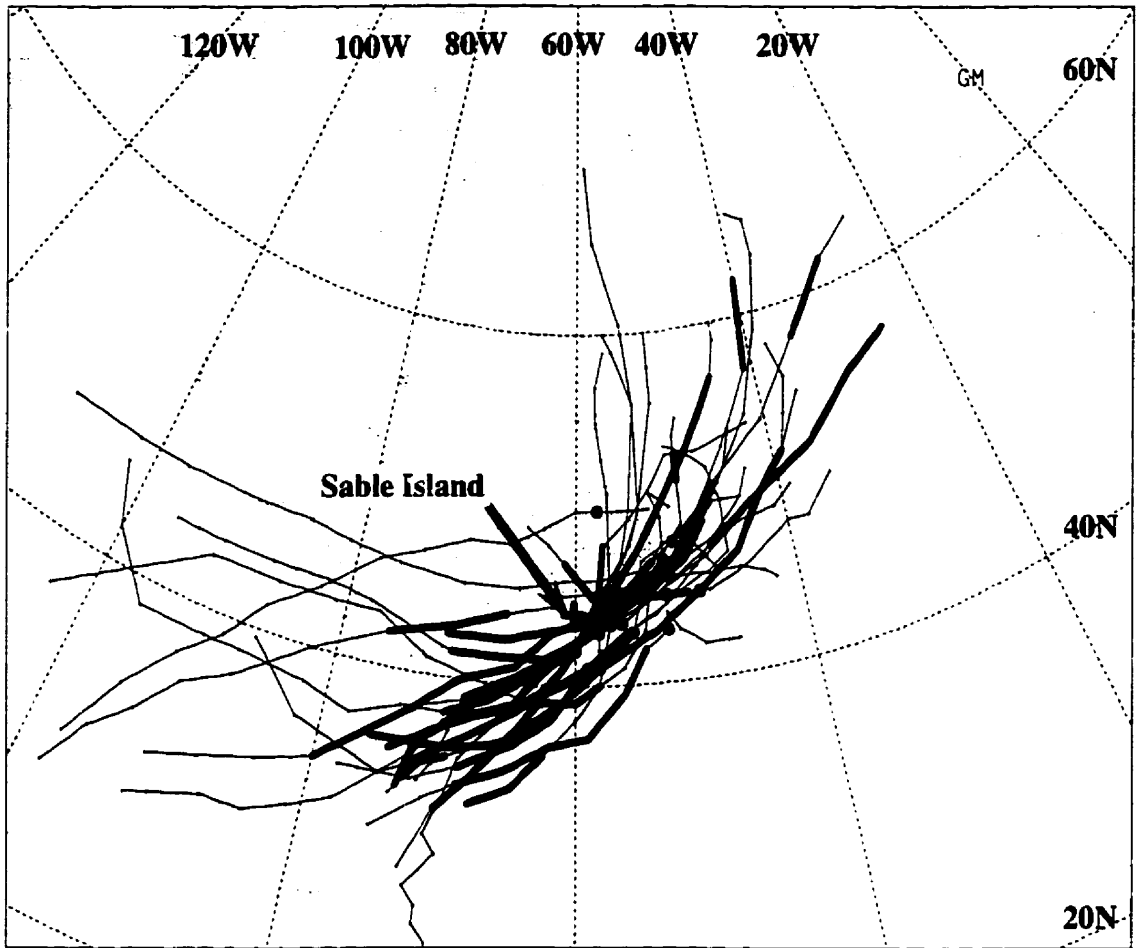


Fig. 4.9 As in fig. 4.2. but for 24 cyclones in NW group A.

longitudes 50-60°W. The overland track of 10 of these cyclones may explain in part the high variance in wind speed in Fig. 3.8 in the 12 hours prior to the peak wind observations at Sable Island. Most of these systems, upon crossing the coastline, tracked east of Sable Island and Newfoundland and curved north towards Greenland.

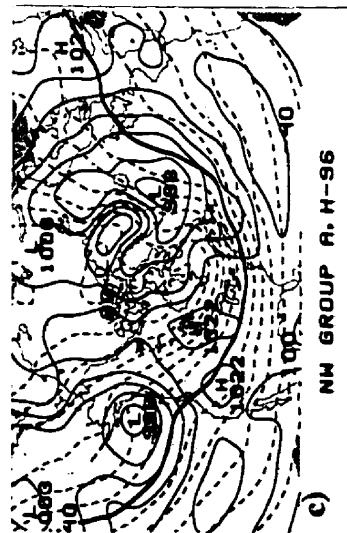
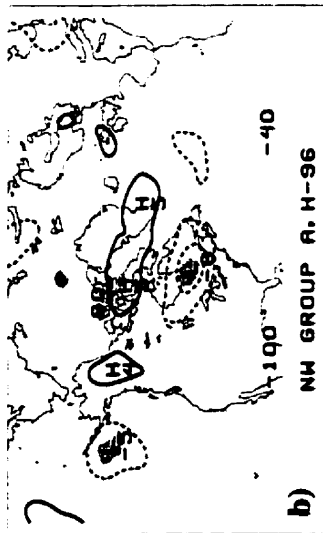
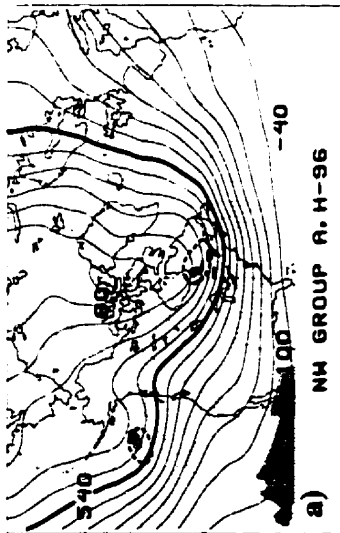
The northward extent of many of these tracks is noteworthy. Seven cyclones managed to reach the Arctic Circle (60°N) by H+36, and all but two lay beyond 50°N by this time. The phase speed of these systems attests to this fact, with an average phase speed of  $14.2 \text{ m s}^{-1}$  between H-12 and H+00 (Table 4.6). With the exception of SW group A (in which we took an average of only 11 cases), this is the highest average phase speed among the five groups. This value would be even higher, but for the fact that the four systems possessing a continental track during this time range had phase speeds below  $10 \text{ m s}^{-1}$ . Only one of the cyclones with an oceanic track during this time had a phase speed below  $10 \text{ m s}^{-1}$ . These phase speeds are comparable to that found by Sanders (1986), who stated that oceanic bombs typically had phase speeds of  $18 \text{ m s}^{-1}$ , as compared to an average speed of  $13 \text{ m s}^{-1}$  for cyclones in winter months.

In general these cyclones were deepening (18 of 24)—in many cases explosively—at the time of the highest winds at Sable Island. Nineteen classified as moderate bombs at some stage in their life cycle, with 11 reaching strong bomb status (Sanders 1986).

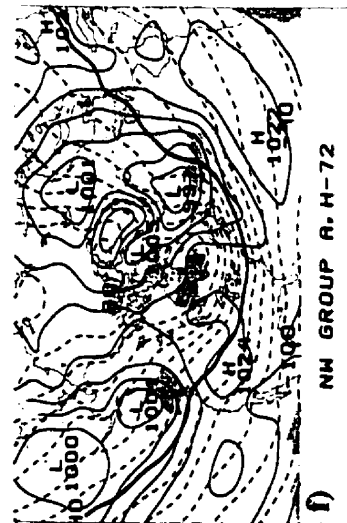
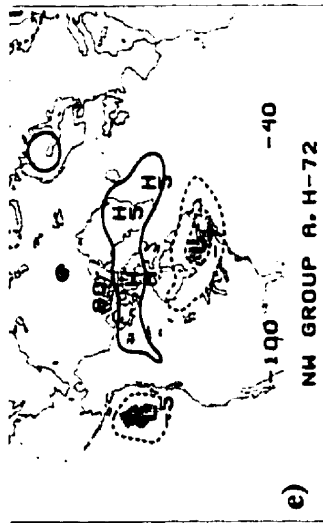
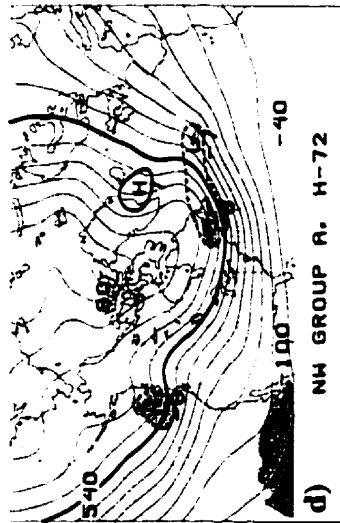
#### *b) Composite evolution of NW group A*

Figure 4.10 gives the six day flow evolution of composite fields associated with the 24 cases in NW group A. The only significant feature at H-96 is a weak cold anomaly north of the Great Lakes. This is related to geostrophic northwesterly flow on the eastern flank of an anticyclone over Manitoba and an upper-level trough over eastern Canada. Over the next two days this cold anomaly drifts eastward to lie over Atlantic Canada at H-48. At this time there is slight evidence of a 500-hPa trough beginning to develop near Lake Michigan, while the Prairie anticyclone has remained nearly stationary. Downstream over the central Atlantic Ocean a significant barotropic ridge is situated over Iceland.

### H-96



### H-72



### H-48

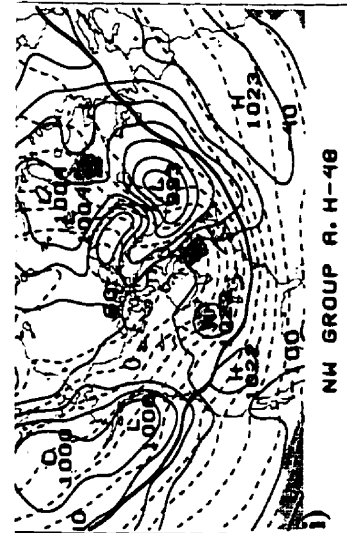
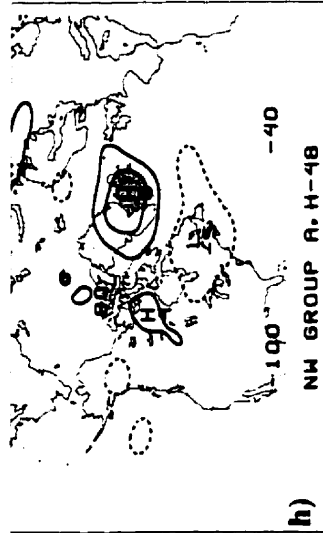
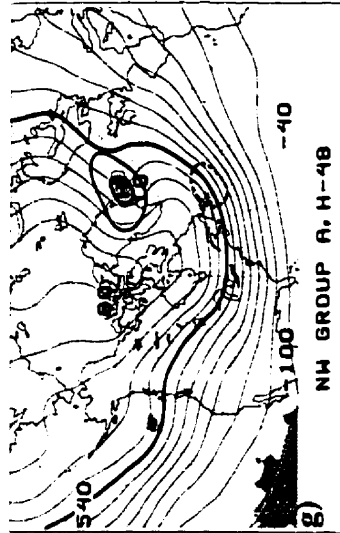
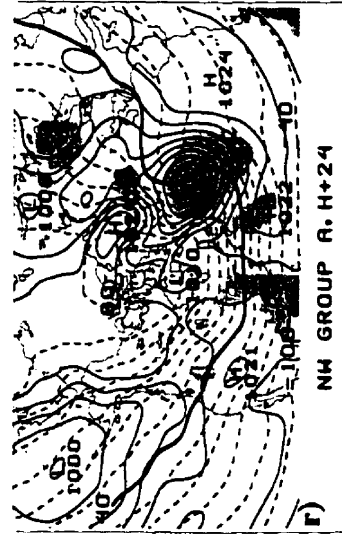
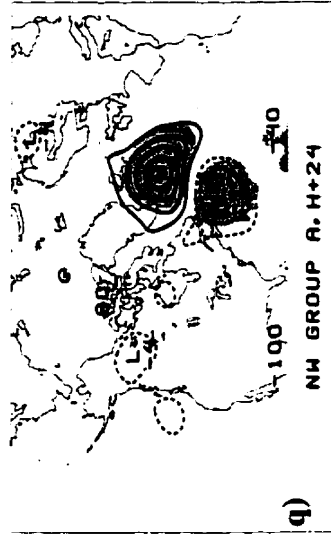
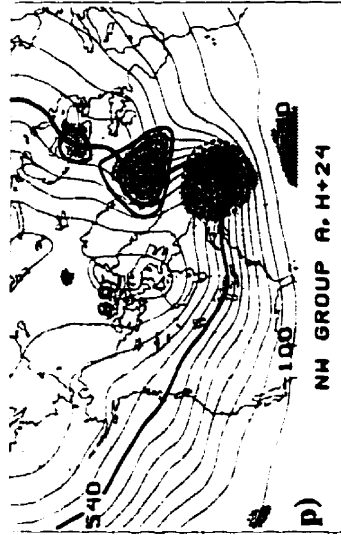
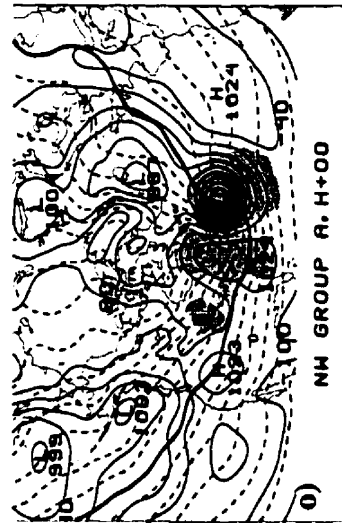
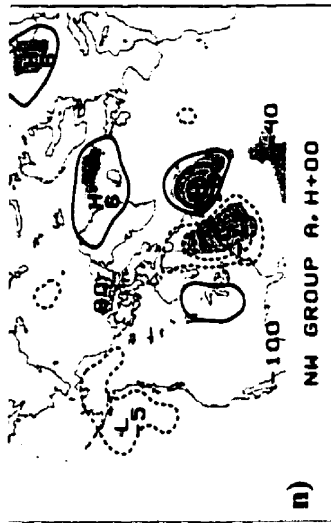
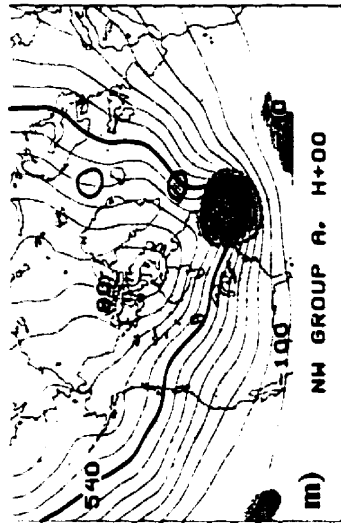


Fig. 4.10 As in fig. 4.3 but for composite of 24 cases in NW group A.

H+24



H+00



H-24

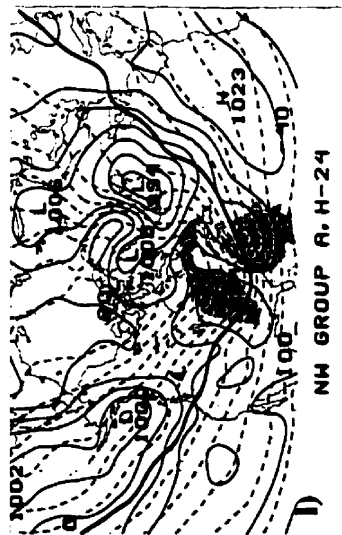
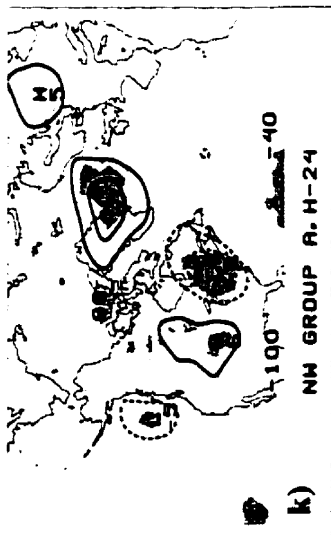
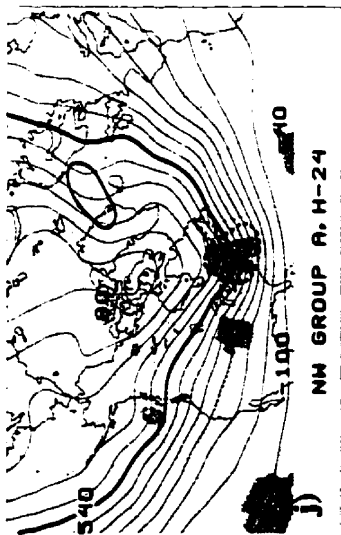


Fig. 4.10 (continued)

Table 4.6 As in Table 4.2 but for NW group A.

NW-Group A							
Date in UTC			peak speed of wind	deepening rate	deepening rate	phase speed	
year	day	month	hour	( $\text{m s}^{-1}$ )	(H-12 - H+00) (hPa/12h)	(H+00 - H+12) (hPa/12h)	(H-12 - H+00) ( $\text{m s}^{-1}$ )
1979	20	January	12	21.1	3.6	5.7	5.4
1980	03	January	18	22.5	-7.6	-7.3	15.5
1980	11	February	06	23.1	-23.8	-12.7	20.7
1980	19	November	12	23.6	-17.5	-12.2	15.4
1981	31	December	12	20.6	0.0	1.2	3.4
1983	07	January	06	23.6	-12.2	-14.2	22.9
1983	13	February	06	25.8	-10.2	-11.0	14.4
1983	27	February	12	21.7	1.2	0.0	9.0
1984	10	March	12	23.6	-6.2	-3.5	12.2
1986	20	November	00	23.1	-10.2	-4.9	22.0
1987	30	December	12	27.8	-12.2	-3.5	18.2
1988	09	March	00	22.2	-10.2	0.0	10.9
1988	22	November	12	20.6	-9.6	-6.0	18.2
1989	05	January	00	23.6	-1.3	0.0	17.4
1989	29	December	12	19.2	-28.2	-27.2	19.8
1991	11	January	00	21.1	-32.8	-30.5	19.8
1992	06	February	06	20.6	-6.3	-4.9	14.2
1992	22	March	12	23.1	5.0	3.5	14.1
1992	07	April	00	23.1	1.3	2.5	1.9
1994	08	November	06	20.0	-4.5	-6.8	8.7
1994	09	December	00	23.1	-20.8	1.2	10.9
1995	11	September	00	21.7	-14.0	-15.1	18.8
1995	27	November	00	24.7	-6.5	-2.4	13.0
1995	03	December	06	20.6	3.6	5.7	5.4

One day before the highest northwest winds at Sable Island the upper-level trough has reached the east coast as a surface cyclone develops east of Cape Hatteras and a shallow anticyclone trails farther west. At this stage the upper trough is not particularly deep. Of the three wind quadrants previously considered at this composite time, this rates as the weakest anomaly (-9 dam). Its nearest rival in the other groups at this time was a negative 14 dam anomaly in both the NE and SE group A (Figs. 4.3j and 4.5j). However, in the next 24 hours rapid deepening occurs at all levels, with explosive composite deepening at the surface and a 14 dam height fall at 500-hPa—the greatest composite height fall at that level of any group. This is an indication that there is strong interaction between upper and lower levels at this time. The upper-level short-wave has progressed rapidly eastward as its half wavelength decreases with the amplification of the downstream ridge.

By H+24 the thermal wave has strongly amplified in the presence of warm-air advection as the upper-level trough progresses east of Newfoundland. The positive 14 dam thickness anomaly is comparable to SE group A at this time (a +17 dam anomaly in Fig. 4.5f). Overall baroclinicity is still strong, even though the composite cyclone has started to fill. The warm air advection has built a high amplitude ridge northeast of 40°W as the upper level pattern over the central North Atlantic and western Europe becomes highly meridional. By contrast the westerly flow aloft over eastern North America has become quite zonal.

The evolution of NW HWEs discussed above suggests that these windstorms are simply classic marine cyclones which develop explosively as an upper-level relative vorticity maximum crosses the east coast (Manobianco 1989). There does not appear to be a dominant signal several days beforehand, as seen in the other groups studied here. However, as found by L96, there appears to a planetary-scale trough anchored over the cyclogenetic region through which smaller-scale transient short-wave troughs propagate rapidly northeastward. This rapid progression is facilitated by the strong zonal flow between 40-90°W, which allows these systems to travel farther offshore as they develop rapidly off the coast. Though they do not appear to be a great threat to the populated

areas along the southeastern USA coast, they can pose serious hazards to marine interests and may also be a threat to Newfoundland.

The implication is that these cyclones would be particularly difficult to forecast. We have demonstrated that there is a lack of strong upper-level signals beforehand that would serve as warning signal. Moreover, the increased phase speeds, rapid upper- and low-level development, and small scales, all combine to make these a forecasting challenge. The movement of cold air over the warm coastal waters (Fig. 4.10d) may also play an important role in many of these systems. Staley and Gall (1977) found that reducing the static stability in the lower troposphere shifts the wavelength of maximum instability towards shorter wavelengths. Since the scale of the 500-hPa trough found in our composite was small throughout the life cycle of the cyclone, reduced static stability may have played a role in the rapid development. The scale of this trough is much smaller than that found in our SW group A composite evolution, which had a closed 500-hPa vortex imbedded in a planetary-scale trough.



## **Chapter 5 - Summary and conclusions**

### **5.1 Summary**

High wind events (HWEs) affecting Atlantic Canada during the period 1979-1995 were studied using wind data at Halifax and Sable Island. A climatology of HWEs was constructed, revealing that these are primarily a cold season event typically occurring between November and April. Throughout the 1980s there was substantial interannual variability in the number of these wind storms. In particular, there were six HWEs at Sable Island in January 1982, twice as many as any other month during our period of study. By contrast, there were no HWEs at Sable Island in January 1984.

Further examination of these contrasting months revealed that the large-scale circulation over the Atlantic ocean may be an important factor in the number of dangerous storms affecting Atlantic Canada. The active month of January 1982 was characterised by weak circulation over the north-central Atlantic Ocean in association with a weakening of the Icelandic Low. The flow over this region resembled that of the negative phase of the NAO. January 1982 was also characterised by a month long cold air surge over western Canada. By contrast, January 1984 had very strong North Atlantic circulation in association with an enhanced Icelandic Low resembling that of the positive phase of the NAO.

Because of the strength and number of HWEs affecting Sable Island and the danger this posed to the marine community, all HWEs affecting this station were chosen as the basis of a study which examined the planetary- and synoptic-scale environment of HWEs. The objective was to determine whether significant signals in the atmosphere could be found several days before high winds affected Sable Island.

High wind events were divided into four groups based on their wind direction falling into one of the four wind quadrants. Distinct differences among these four groups emerged based on the results of a linear correlation analysis which was applied to the 1000-hPa geopotential height anomaly fields for HWEs in each wind quadrant. The main results are summarised below.

*a) NE quadrant*

In comparison to the other three wind quadrants in this study, NE HWEs are characterised by the weakest thermal gradients and weakest upper-level forcing. Related to this was the finding that they are generally slow moving cyclones which are either filling or deepening slowly as they pass southeast of Sable Island at the time of the highest winds. One of the possible explanations for their weak dynamical structure is the finding that NE HWEs frequently occur in months outside the traditional winter period of December-February.

The offshore track with a strong easterly component was related to an anticyclone situated over northern Quebec at H+00 which helped keep the cyclone responsible for the high winds well offshore. This anticyclone had formed over northern Ontario at H-72 and tracked to the east, strengthening as it went. It appeared to develop in conjunction with the cyclone over the southeastern United States as the flow gradually began to split at 500-hPa.

The most significant upper-level signature found was a prominent area of ridging extending from Iceland to Baffin Island at H-96. This anomaly remained quasi-stationary throughout the composite evolution and was found to persist as far back as H-160. A ridge anomaly was seen in these regions in each of the other quadrants at various times during the respective composite evolutions and supports the finding of January 1982 in which six HWEs occurred during a month with an anomalously weak Icelandic Low. However, in the NE quadrant this anomaly appeared to be independent of the development of the composite cyclone and retained its significance for a much longer period of time than the other quadrants. This suggests its importance as a precedent signal to NE HWEs.

One other important signal prior to the HWE was the presence of a significant east coast upper-level cold trough and surface cyclone at H-96. This upper-level trough appeared to propagate across the Atlantic along 45°N in split Atlantic flow. Meanwhile the cyclogenetic upper-level trough propagated in from the Pacific ocean, crossing the southern States and strengthening as it passed near the Gulf of Mexico.

Storms in the NE quadrant qualitatively fit the Davis et al. (1993) description of a “Florida low”. These authors reported that Florida lows are blocked by an anticyclone to the north, are slow moving and exhibit northeast to southwest elongation. They also found that in many cases the upper-level flow was split and cyclones stalled over the Atlantic because of weak upper-level steering currents. Davis et al (1993) also stated that from a seasonal perspective “Florida lows” occurred most frequently in March, in agreement with Klein (1957). It is significant that all these features are characteristic of NE HWEs and that the month these occurred in most frequently was March (8 of 30).

*b) SE quadrant*

Peak winds from the southeast at Sable Island were on average the weakest of any direction and occurred the least frequently. The strong winds were identified to be primarily the result of a strong pressure gradient between a cyclone to the west of Sable Island and a downstream anticyclone. As the cyclone tracked rapidly northward over land and cyclonic vorticity advection was reduced with the growth of a downstream ridge, winds in this quadrant generally weakened quickly over Sable Island. It was the growth and subsequent decline in speed of the eastward propagation of the downstream ridge that influenced the strong northern component in the tracks of many of these cyclones.

The most important predecessor signal to SE HWEs was the presence of two anticyclones at H-96—one over southern Manitoba and a second one in the eastern Pacific west of southern California. The former was an integral component in the breakdown of fast zonal flow over the continent at H-48. The anticyclone west of California appeared to redevelop over Nevada and helped to amplify the quasi-stationary ridge over western North America (Lackmann et al. 1996), favouring the genesis of a trough which would eventually sustain the cyclone at H+00. There was also a prominent planetary-scale trough at 500-hPa over eastern Canada at H-96 which supported a significant east coast cyclone and cold air over much of the region.

The anticyclone which travelled southeast from the Prairies into the Atlantic acted to amplify the thermal wave between it and the developing cyclone. The result was

tremendous growth of the downstream ridge over the Atlantic ocean. This may be an important mechanism in the development and sustainment of blocking ridges sometimes seen over the central Atlantic (Mullen 1987). This ridge was also a significant factor in the rapid weakening of the cyclone on the east coast.

Is the anticyclone just as important as forcing from an upper-level trough for cyclones in the SE quadrant? The evidence seems to support this conjecture. A fast upper-level meridional pattern develops as cyclone-anticyclone pairs perturb the thermal wind and sustain developing baroclinic instability during SE HWEs. However, what serves to initially favour cyclonic development eventually acts to restrict it, as the downstream ridge grows in amplitude and slows the eastward progression of the wave.

*c) SW quadrant*

This was the most difficult of the four quadrants to generalise. On average the peak winds of SW HWEs were the strongest. However, there was wide variation in the types of weather systems responsible for these winds. Our linear correlation analysis yielded two groups which differed from each other mainly in the paths of the cyclones and their positions at H+00.

The key link in both groups was the intensity of the cold surge attendant with the high winds at Sable Island. Marine systems in group A developed explosively as a region of cold air in association with a large-scale digging trough reached the coast. This agrees with Konrad and Colucci's (1989) finding that the strong coastal cyclones tend to follow, rather than precede, intense cold surges. As explosive development occurred (the composite cyclone deepened 24 hPa in 24 hours), the cyclones closely followed the coastline as they moved rapidly to lie near Sable Island at H+00.

Despite their explosive nature, there were clear atmospheric signals four days before SW HWEs in group A. The pattern over the eastern Pacific and western North America resembled that of the positive phase of the PNA pattern. Moreover, the enhanced west coast ridge at this time acted as a favourable mechanism for a developing

cold air surge. This serves to reinforce what was found in January 1982--that cold air surging towards the east coast is an important forerunner of very intense storms.

The second group of SW HWEs (group B) were much more difficult to generalise, though 7 of these 9 systems followed a continental storm track. Sometimes high winds from the southwest at Sable Island are due to cyclonic flow related to a low pressure system as far north as the Labrador Sea and sometimes even the Arctic Circle. With more confidence it can be said that a low frequency cold surge is often in place over much of the northern United States and Canada at H+00 during SW HWEs.

*d) NW quadrant*

Weather systems giving strong northwest winds to Sable Island were generally deepening, many explosively, as they tracked near the Gulf Stream to lie east of Sable Island at H+00. Related to this rapid deepening was the high phase velocity of many of these cyclones. Wind magnitudes were generally large in the hours following the peak wind speed as the cyclones curved to the north and continued to deepen as they passed the island.

The fast propagation, explosive nature, and strength and duration of winds associated with these cyclones make them particularly dangerous. This is in addition to the fact that composites based on the linear correlation analysis show they are the most difficult to find signals for several days ahead of time. Between H-96 and H-48 the only significant feature over North America was a weak cold trough over southern Quebec and the Atlantic provinces. It was only out of a broad planetary-scale trough that a rapidly travelling short-wave became apparent at H-24. The associated surface- and upper-level trough then simultaneously developed at all levels in the hours leading up to H+00.

Findings in the NW quadrant demonstrate that there is a class of explosive cyclones for which there are no evident predecessor atmospheric signals. These may be among the marine systems which numerical weather prediction models frequently have such a difficult time forecasting.

## 5.2 Conclusions

Very different atmospheric signals have been found to have important impacts on the track, development, and strength of dangerous storms affecting Sable Island. These signals have been found to be coherent and well-defined several days before the occurrence of a HWE. Studies such as this one may be useful in improving long range probability forecasts of dangerous windstorms. However, the finding that clear signals were absent in the NW quadrant highlights the inherent unpredictability of many dangerous marine systems and suggests that these particular storms deserve special attention.

Though not shown, a similar analysis was performed for Halifax and found circulation patterns unique from those of Sable Island. It emphasises the importance of studies such as this one for regional forecasting. Though the synoptic scale is on the order of thousands of kilometres, slight differences in a cyclone's track can have devastating consequences, both in terms of economics and in terms of loss of life.

Certain well known teleconnection patterns such as the NAO and PNA patterns may have important implications for studies such as this one. It is a significant fact that not one of the composite fields had an enhanced Icelandic Low in its climatological position. The enhanced positive phase of the NAO may be an important factor in inhibiting strong cyclonic development along the east coast.

## REFERENCES

- Avila, L. A., and R. J. Pasch, 1992: North Atlantic Hurricanes\_1991. *Mar. Wea. Log*, **36**, 14-20.
- Balasubramanian, G., and M. K. Yau, 1994: The effects of convection on a simulated marine cyclone. *J. Atmos. Sci.*, **51**, 2397-2417.
- Basist, A. N., and M. Chelliah, 1997: Comparison of tropospheric temperatures derived from the NCEP/NCAR reanalysis, NCEP operational analysis, and the microwave sounding unit. *Bull. Amer. Meteor. Soc.*, **78**, 1431-1447.
- Bell, G. D., and L. F. Bosart, 1989: The large-scale atmospheric structure accompanying New England coastal frontogenesis and associated North American east coast cyclogenesis. *Quart. J. Roy. Meteor. Soc.*, **115**, 1133-1146.
- Betts, A. K., S. Hong, and H. Pan, 1996: Comparison of NCEP-NCAR reanalysis with 1987 FIFE data. *Mon. Wea. Rev.*, **124**, 1480-1498.
- Bluestein, H. B., 1993: *Synoptic-Dynamic Meteorology in Midlatitudes*, Vol. II, Oxford University Press, 277-282 pp.
- Bosart, L. F., 1981: The Presidents' Day snowstorm of 18-19 February 1979: A subsynoptic-scale event. *Mon. Wea. Rev.*, **109**, 1542-1566.
- \_\_\_\_\_, and S. C. Lin, 1984: A diagnostic analysis of the Presidents' Day storm of February 1979. *Mon. Wea. Rev.*, **112**, 2148-2177.
- Browning, K. A., and N. M. Roberts, 1994: Structure of a frontal cyclone. *Quart. J. Roy. Meteor. Soc.*, **120**, 1535-1557.
- Chou, S.-H., and D. Atlas, 1982: Satellite estimates of ocean-air heat fluxes during cold air outbreaks. *Mon. Wea. Rev.*, **110**, 1434-1450.
- Climate Perspectives, 1982: **4**, No. 2, pp 1; No. 3, pp 1.

Davis, R. E., and R. Dolan, 1992: The "All-Hallows' Eve coastal storm"—October 1991. *J. Coastal Res.*, **8**, 239-243.

\_\_\_\_\_, \_\_\_\_\_, and G. Demme, 1993: Synoptic climatology of Atlantic Coast northeasters. *Int. J. Climatol.*, **13**, 171-188.

desJardins, M. L., K. F. Brill, and S. S. Schotz, 1991: Use of GEMPAK on UNIX workstations. *Proc. Seventh Int. Conf. on Interactive Information and Processing Systems for Meteorology, Oceanography, and Hydrology*, New Orleans, LA, Amer. Meteor. Soc., 449-453.

Dickson, R. R. and J. Namais, 1976: North American influences on the circulation and climate of the North Atlantic sector. *Mon. Wea. Rev.*, **10**, 1255-1264.

Dole, R. M., 1986: Persistent anomalies of the extratropical northern hemisphere wintertime circulation: structure. *Mon. Wea. Rev.*, **114**, 178-207.

Frederikson, J. S., 1979a: The effects of long planetary waves on the regions of cyclogenesis: Linear theory. *J. Atmos. Sci.*, **36**, 195-204.

Gutowski, W.J., Y. Chen, and Z. Otles, 1997: Atmospheric water vapour transport in NCEP-NCAR reanalysis: Comparison with river discharge in the central United States. *Bull. Amer. Meteor. Soc.*, **78**, 1957-1969.

Gyakum, J. R., 1983a: On the evolution of the *QEII* storm. Part I: Synoptic aspects. *Mon. Wea. Rev.*, **111**, 1137-1155.

\_\_\_\_\_, 1983b: On the evolution of the *QEII* storm. Part II: Dynamic and thermodynamic structure. *Mon. Wea. Rev.*, **111**, 1156-1173.

\_\_\_\_\_, D. Zhang, J. Witte, K. Thomas, and W. Wintels, 1996: CASP II and the Canadian cyclones during the 1989-92 cold seasons. *Atmos.-Ocean*, **34**, 1-16.

Hadlock, R., and C. W. Kreitzberg, 1988: The Experiment on Rapidly Intensifying Cyclones over the Atlantic (ERICA) field study - Objectives and plans. *Bull. Amer. Meteor. Soc.*, **69**, 1309-1320.



- Kalnay, E., M. Kanamitsu, R. Kistler, W. Collins, D. Deaven, L. Gandin, M. Iredell, S. Saha, G. White, J. Woollen, Y. Zhu, M. Chelliah, W. Ebisuzaki, W. Higgins, J. Janowiak, K. C. Mo, C. Ropelewski, J. Wang, A. Leetmaa, R. Reynolds, R. Jenne, and D. Joseph, 1996: The NCEP/NCAR 40-year reanalysis project. *Bull. Amer. Meteor. Soc.*, **77**, 437-471.
- Khandekar, M. L., and V. R. Swail, 1995: Storm waves in Canadian waters: A major marine hazard. *Atmos.-Ocean*, **33**, 329-357.
- Klein, W. H., 1957: *Principal tracks and mean frequencies of cyclones and anticyclones in the Northern Hemisphere*. US Department of Commerce Research Paper No. 40, Washington, DC, 60 pp.
- Konrad, C. E., 1996: Relationships between the intensity of cold-air outbreaks and the evolution of synoptic and planetary-scale features over North America. *Mon. Wea. Rev.*, **124**, 1067-1083.
- \_\_\_\_\_, and Colucci, 1989: An examination of extreme cold air outbreaks over eastern North America. *Mon. Wea. Rev.*, **117**, 2687-2700.
- Kuo, Y., R. J. Reed, and S. Low-Nam, 1991: Effects of surface energy fluxes during the early development and rapid intensification stages of seven explosive cyclones in the Western Atlantic. *Mon. Wea. Rev.*, **119**, 457-476.
- Lackmann, G. M., L. F. Bosart, and D. Keyser, 1996: Planetary- and synoptic-scale characteristics of explosive wintertime cyclogenesis over the western North Atlantic Ocean. *Mon. Wea. Rev.*, **124**, 2672-2702.
- Lau, N., 1988: Variability of the observed midlatitude storm tracks in relation to low-frequency changes in circulation pattern. *J. Atmos. Sci.*, **45**, 2718-2743.
- Lund, I. A., 1963: Map-pattern classification by statistical methods. *J. Appl. Meteor.*, **2**, 56-65.
- Manobianco, J., 1989: Explosive East Coast cyclogenesis over the West-Central North Atlantic Ocean: A composite study derived from ECMWF operational analysis. *Mon. Wea. Rev.*, **117**, 2365-2383.

- Mo, K. C., and R. W. Higgins, 1996: Large-scale atmospheric moisture transport as evaluated in the NCEP/NCAR and the NASA/DAO reanalysis. *J. Climate*, **9**, 1531-1545.
- Mullen, S. L., 1987: Transient eddy forcing of blocking flows. *J. Atmos. Sci.*, **44**, 3-22.
- Murty, T. S., S. Venkatesh, M. B. Danard, and M. I. El-Sabh, 1995: Storm surges in Canadian waters. *Atmos.-Ocean*, **33**, 359-387.
- Panofsky, H. A., and G. W. Brier, 1968: *Some Applications of Statistics to Meteorology*. The Pennsylvania State University Press, 224 pp.
- Petterssen, S., 1956: *Weather Analysis and Forecasting*, Vol. 1, 2d ed. McGraw-Hill, 428 pp.
- Quiroz, R. S., 1984: The climate of the 1983-84 winter—A season of strong blocking and severe cold in North America. *Mon. Wea. Rev.*, **112**, 1894-1912.
- Rausch, R. L., and P. J. Smith, 1996: A diagnosis of a model-simulated explosively developing extratropical cyclone. *Mon. Wea. Rev.*, **124**, 875-904.
- Reed, R. J., and M. D. Albright, 1986: A case study of explosive cyclogenesis in the eastern Pacific. *Mon. Wea. Rev.*, **114**, 2297-2319.
- Reitan, C. H., 1974: Frequencies of cyclones and cyclogenesis for North America, 1951-1970. *Mon. Wea. Rev.*, **10**, 861-868.
- Roebber, P. J., 1984: Statistical analysis and updated climatology of explosive cyclones. *Mon. Wea. Rev.*, **112**, 1577-1589.
- \_\_\_\_\_, 1993: A diagnostic case study of self-development as an antecedent conditioning process in explosive cyclogenesis. *Mon. Wea. Rev.*, **121**, 976-1006.

- Rogers, J. C., 1990: Patterns of low-frequency monthly sea level pressure variability (1899-1986) and associated wave cyclone frequencies. *J. Climate*, **3**, 1364-1379.
- Rogers, E., and L. F. Bosart, 1986: An investigation of explosively deepening oceanic cyclones. *Mon. Wea. Rev.*, **114**, 702-718.
- Sanders, F., 1986: Explosive cyclogenesis in the west-central North Atlantic Ocean, 1981-1984. Part I: Composite structure and mean behaviour. *Mon. Wea. Rev.*, **114**, 1781-1794.
- \_\_\_\_\_, 1988: Life history of mobile troughs in the upper westerlies. *Mon. Wea. Rev.*, **116**, 2629-2648.
- \_\_\_\_\_ and C. A. Davis, 1988: Patterns of thickness anomaly for explosive cyclogenesis over the west-central North Atlantic ocean. *Mon. Wea. Rev.*, **116**, 2725-2730.
- \_\_\_\_\_ and J. R. Gyakum, 1980: Synoptic-dynamic climatology of the "bomb". *Mon. Wea. Rev.* **108**, 1589-1606.
- Snyder, C., 1996: Summary of an informal workshop on adaptive observations and FASTEX. *Bull. Amer. Meteor. Soc.*, **77**, 953-961.
- Staley, D. O., and R. L. Gall, 1977: On the wavelength of maximum baroclinic instability. *J. Atmos. Sci.*, **34**, 1679-1688.
- Stewart, R. E., 1991: Canadian Atlantic Storms Program: Progress and plans for the meteorological component. *Bull. Amer. Meteor. Soc.*, **72**, 364-371.
- \_\_\_\_\_, D. Bachand, R. R. Dunkley, A. G. Giles, B. Lawson, L. Legal, S. T. Miller, B. P. Murphy, M. N. Parker, B. J. Paruk, and M. K. Yau, 1995: Winter storms over Canada. *Atmos.-Ocean*, **33**, 223-247.
- Stoss, L. A., and S. L. Mullen, 1995: The dependence of short-range 500-mb height forecasts on the initial flow regime. *Wea. Forecasting*, **10**, 353-368.

- Sutcliffe, R. C., and A.G. Forsdyke, 1950: The theory and use of upper air thickness patterns in forecasting. *Quart. J. Roy. Meteor. Soc.*, **76**, 189-217.
- Uccellini, L. W., 1986: The possible influence of upstream upper-level baroclinic processes on the development of the QEII storm. *Mon. Wea. Rev.*, **111**, 1019-1027.
- \_\_\_\_\_, and P. J. Kocin, 1987: An examination of vertical circulations associated with heavy snow events along the East Coast of the United States. *Wea. Forecasting*, **2**, 289-308.
- \_\_\_\_\_, and \_\_\_\_\_, 1990: *Snowstorms along the Northeastern Coast of the United States: 1955 to 1985*. American Meteorological Society, 20 pp.
- \_\_\_\_\_, \_\_\_\_\_, R. A. Petersen, C. H. Wash and K. F. Brill, 1984: The Presidents' Day cyclone of 18-19 February 1979: Synoptic overview and analysis of the subtropical jet streak influencing the pre-cyclogenetic period. *Mon. Wea. Rev.*, **112**, 31-55.
- \_\_\_\_\_, R. A. Petersen, K. F. Brill, P. J. Kocin, and J. J. Tucillo, 1987: Synergistic interactions between an upper level jet streak and diabatic processes that influence the development of a low-level jet and a secondary coastal cyclone. *Mon. Wea. Rev.*, **115**, 2227-2261.
- Wagner, A. J., 1982: Weather and circulation of January 1982—A stormy month with two record cold waves. *Mon. Wea. Rev.*, **110**, 310-317.
- Wallace, J. M., and Gutzler, 1981: Teleconnections in the geopotential height field during the Northern Hemisphere winter. *Mon. Wea. Rev.*, **109**, 784-812.
- Weinstein, A. I., and F. Sanders, 1989: Wind increases in rapid marine cyclogenesis. *Mon. Wea. Rev.*, **117**, 1365-1367.
- Whittaker, L. M., and L. H. Horn, 1984: Northern hemisphere extratropical cyclone activity for four mid-season months. *J. Climatol.*, **4**, 297-310.
- Zhang, D. and K. MacGillivray, 1997: A numerical investigation of a moderate coastal storm with intense precipitation. *Atmos.-Ocean*, **35**, 161-188.

Zishka, K. M. and Smith, P. J., 1980: The climatology of cyclones and anticyclones over North America and surrounding ocean environs for January and July, 1950-77. *Mon. Wea. Rev.*, **108**, 387-401.